



THE CATALYTIC PYROLYSIS OF COCONUT SHELL OVER NI-DOPED ACTIVATED CARBON
CATALYST FOR AROMATIC-RICH BIO-OIL PRODUCTION



By
MR. Iyarin TONGDANG

A Thesis Submitted in Partial Fulfillment of the Requirements
for Master of Engineering CHEMICAL ENGINEERING

Department of CHEMICAL ENGINEERING

Silpakorn University

Academic Year 2022

Copyright of Silpakorn University

ไฟโรไลซิสเชิงเร่งปฏิกิริยาของกะลามะพร้าวด้วยตัวเร่งปฏิกิริยานิกเกิลถ่านกัมมันต์สำหรับ
การผลิตน้ำมันชีวภาพที่มีสารอะโรมาติกสูง



โดย
นายไวยรินทร์ ทองแดง

วิทยานิพนธ์นี้เป็นส่วนหนึ่งของการศึกษาตามหลักสูตรวิศวกรรมศาสตรมหาบัณฑิต

สาขาวิชาวิศวกรรมเคมี แผน ก แบบ ก 2 ระดับปริญญามหาบัณฑิต

ภาควิชาวิศวกรรมเคมี

มหาวิทยาลัยศิลปากร

ปีการศึกษา 2565

ลิขสิทธิ์ของมหาวิทยาลัยศิลปากร

THE CATALYTIC PYROLYSIS OF COCONUT SHELL OVER NI-DOPED ACTIVATED
CARBON CATALYST FOR AROMATIC-RICH BIO-OIL PRODUCTION



By
MR. Iyarin TONGDANG

A Thesis Submitted in Partial Fulfillment of the Requirements
for Master of Engineering CHEMICAL ENGINEERING
Department of CHEMICAL ENGINEERING
Silpakorn University
Academic Year 2022
Copyright of Silpakorn University

Title THE CATALYTIC PYROLYSIS OF COCONUT SHELL OVER NI-DOPED
ACTIVATED CARBON CATALYST FOR AROMATIC-RICH BIO-OIL
PRODUCTION

By MR. Iyarin TONGDANG

Field of Study CHEMICAL ENGINEERING

Advisor Associate Professor Worapon Kiatkittipong, D.Eng.

Co advisor Associate Professor Ekrachan Chaichana, D.Eng.

Faculty of Engineering and Industrial Technology, Silpakorn University in Partial
Fulfillment of the Requirements for the Master of Engineering

..... Dean of Faculty of
(Assistant Professor Arunsri Leejeerajumnian) Engineering and Industrial
Technology

Approved by

..... Chair person
(Assistant Professor Tarawipa Puangpetch, D.Eng.)

..... Advisor
(Associate Professor Worapon Kiatkittipong, D.Eng.)

..... Co advisor
(Associate Professor Ekrachan Chaichana, D.Eng.)

..... Committee
(Assistant Professor Nutchapon Chotigkrai, D.Eng.)

..... External Examiner
(Assistant Professor Adisak Jaturapiree, Dr.rer.nat.)



61404203 : Major CHEMICAL ENGINEERING

Keyword : Biomass; catalytic pyrolysis; bio-oil upgrading; Ni modification; aromatic hydrocarbon

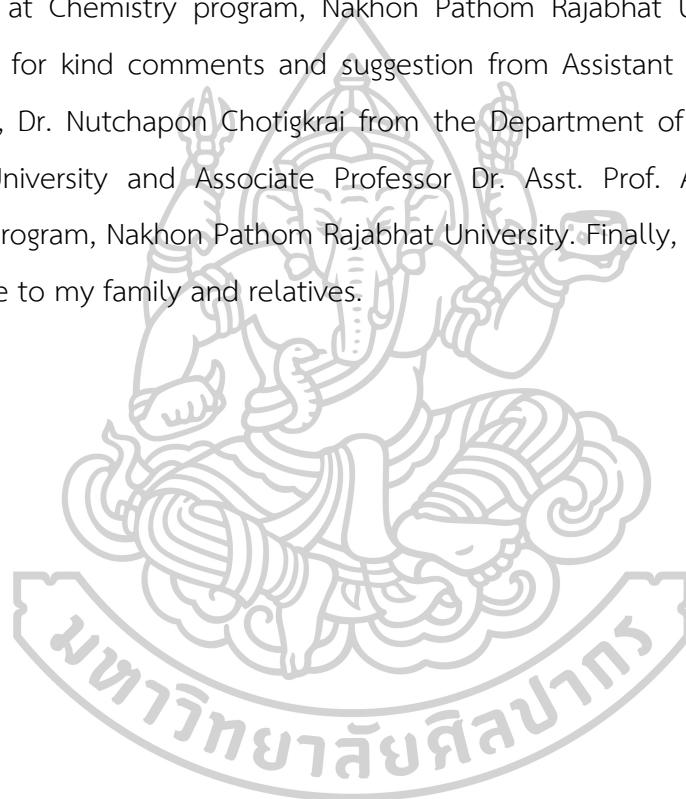
MR. Iyarin TONGDANG : THE CATALYTIC PYROLYSIS OF COCONUT SHELL OVER Ni-DOPED ACTIVATED CARBON CATALYST FOR AROMATIC-RICH BIO-OIL PRODUCTION Thesis advisor : Associate Professor Worapon Kiatkittipong, D.Eng.

The coconut shell (CS) was utilized as biomass feedstock for aromatic-rich bio-oil production. Commercial activated carbon was modified with 5-20 wt.% of Ni loading using wet impregnation method and applied in the catalytic pyrolysis of coconut shell for upgrading bio-oil. The synthesized catalysts were characterized by N₂ adsorption-desorption (Brunauer-Emmett-Teller, BET), X-ray diffractometer (XRD) and X-ray fluorescence (XRF). According to the obtained results, the prepared catalysts have a surface area and pore size in the range of 470-630 m²/g and 3.92-6.44 nm, respectively. Fourier transform infrared spectroscopy (FTIR) method was used to characterize the different functional groups of raw coconut shell and coconut biochar after pyrolysis. The components of pyrolysis bio-oil were analyzed by Gas Chromatography – Mass Spectrometry (GC-MS). Under non-catalytic thermal pyrolysis, the pyrolysis temperature of 400 °C could maximize the bio-oil yield of 49.0%. Phenolic compounds (approx. 58.8%) was obtained as a main component in the thermal pyrolysis bio-oil. Bio-char yield could be promoted at lower pyrolysis temperature of 300 °C while the gas products are promoted at higher temperature of 500 °C. For catalytic upgrading, several reactions including deoxygenation, decarboxylation, dehydration and polymerization were promoted; however, the bio-oil yield decreased with increasing Ni loading due to the promotion of secondary reactions. The catalysts with 10 wt.% Ni loading exhibited the highest hydrocarbon content of 67.1% which almost all is aromatic hydrocarbon and small amount of aliphatic hydrocarbon with bio-oil yield of 42.66 %. The aromatic selectivity in the upgraded bio-oil was in the order of toluene > benzene > xylene > ethylbenzene. This study provided a potential strategy for aromatic-rich bio-oil production with low-cost and effective production.



ACKNOWLEDGEMENTS

The author would like to express gratitude and appreciation to adviser, Assoc. Prof. Worapon Kiatkittipong for his kind support and recommendations and conversations. This research would not have been completed if I do not have this support. In addition, author would like to thank my co-advisor, Asst. Prof. Ekrachan Chaichana for her support, and guidelines. I also thank for the funding and location for experiment at Chemistry program, Nakhon Pathom Rajabhat University. Author also appreciated for kind comments and suggestion from Assistant Professor Dr. Tarawipa Puangpetch, Dr. Nutchapon Chotigkrai from the Department of Chemical Engineering, Silpakorn University and Associate Professor Dr. Asst. Prof. Adisak Jaturapiree from Chemistry program, Nakhon Pathom Rajabhat University. Finally, I would like to express my gratitude to my family and relatives.



MR. Iyarin TONGDANG

TABLE OF CONTENTS

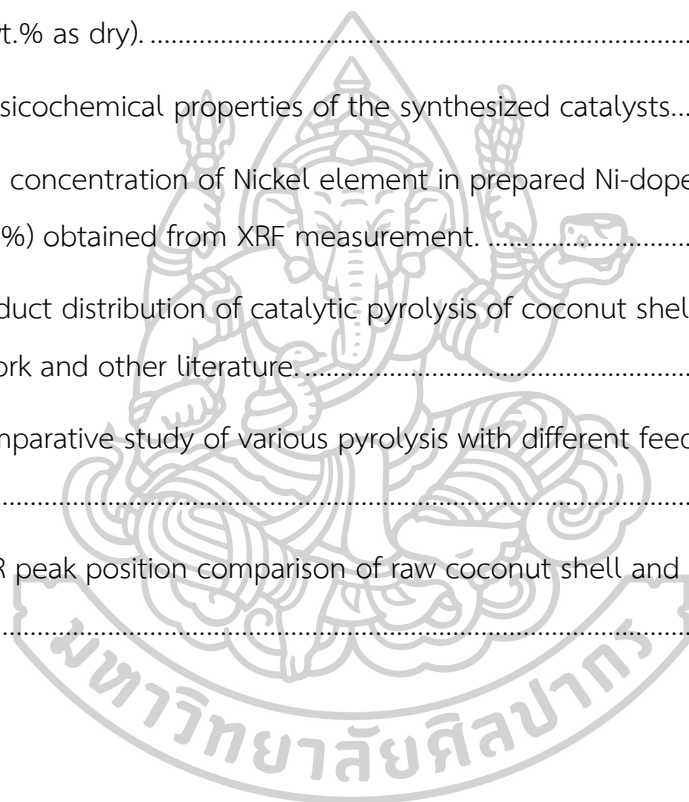
	Page
ABSTRACT	D
ACKNOWLEDGEMENTS	F
TABLE OF CONTENTS	G
LIST OF TABLES	H
LIST OF FIGURES	I
CHAPTER 1	1
INTRODUCTION	1
1.1 Motivation	1
1.2 The objectives of Research	3
1.3 Scopes of Research	3
1.4 Experimental locations	3
Chapter 2	4
Literature Reviews	4
2.1 Biomass	4
2.2 Coconut shell	5
2.3 Pyrolysis process	6
2.4 Type of pyrolysis process	8
2.5 Pyrolysis of Biomass composition	12
2.6 Pyrolysis reactor	15
2.7 Catalyst	25
Chapter 3	32

Theory.....	32
3.1 Pyrolysis behavior of lignocellulose biomass.....	32
3.2 Pyrolysis process model.....	34
Chapter 4.....	40
Methodology.....	40
4.1 Chemical.....	40
4.2 Instruments.....	40
4.3 Feedstock preparation and characterization.....	40
4.4. Catalyst preparation and characterization.....	42
4.5. Experimental procedure.....	45
4.6. Analysis of bio-oil and biochar.....	46
Chapter 5.....	47
Results and Discussion.....	47
5.1 Characterization of Feedstock.....	47
5.2 Characterization of Catalyst.....	49
5.3 Thermal pyrolysis.....	51
5.4 Catalytic pyrolysis.....	52
5.5 Characterization of Biochar.....	61
Chapter 6.....	63
Conclusions.....	63
5.1 Conclusion.....	63
5.2 Suggestion.....	64
Appendix.....	66
REFERENCES.....	69



LIST OF TABLES

Table 1 Some chemicals found in bio-oils [18].	10
Table 2 The reactor type, bio-oil production, and applications.	21
Table 3 Processes for the thermochemical conversion of biomass.....	23
Table 4 Proximate and ultimate analysis of coconut shell from this work and literature (wt.% as dry).	48
Table 5 Physicochemical properties of the synthesized catalysts.....	49
Table 6 The concentration of Nickel element in prepared Ni-doped activated carbon catalyst (wt.%) obtained from XRF measurement.	51
Table 7 Product distribution of catalytic pyrolysis of coconut shell without catalyst from this work and other literature.....	54
Table 8 Comparative study of various pyrolysis with different feedstock, catalyst, and conditions.....	59
Table 9 FTIR peak position comparison of raw coconut shell and other biochar after pyrolysis.....	62



LIST OF FIGURES

Figure 1 Diagram of catalytic pyrolysis of biomass for producing high-quality liquid fuels and chemicals using various catalysts.	3
Figure 2 The major components of biomass [6].	5
Figure 3 The coconut productivity of Nakhon Pathom.	6
Figure 4 Thermal decomposition process of biomass.	7
Figure 5 Fast pyrolysis process [19].	11
Figure 6 Ablative reactor.	15
Figure 7 Rotating cone reactor [29].	16
Figure 8 fluidized bed reactor [30].	17
Figure 9 Circulating fluids bed reactor [32].	18
Figure 10 Entrained flow reactor [33].	19
Figure 11 The vacuum moving bed reactor [37].	20
Figure 12 Pyrolysis behavior of cellulose [6].	33
Figure 13 Pyrolysis behavior of lignin [6].	34
Figure 14 The experiment setup of catalytic pyrolysis of coconut shell.	46
Figure 15 The XRD pattern of obtained Ni-doping activated carbon catalysts.	50
Figure 16 Thermal pyrolysis of coconut shells at 300, 400 and 500 °C.	52
Figure 17 Mass balance of product yields obtained from pyrolysis/deoxygenation of coconut shell over 0-20%Ni-activated carbon catalyst at 400 °C.	53
Figure 18 The chemical compositions of bio-oil obtained from pyrolysis/deoxygenation of coconut shell over 0-20%Ni-activated carbon catalyst. ..	55
Figure 19 Aromatic selectivity of bio-oil obtained from pyrolysis/deoxygenation of coconut shell over 0-20%Ni-activated carbon catalyst.	57

Figure 20 FTIR spectra of raw coconut shell and coconut chars with pyrolysis
temperature, 400 °C..... 61



CHAPTER 1

INTRODUCTION

1.1 Motivation

The rising population nowadays has accompanied the increasing industrial and commercial activities in this world, leading to high energy demand and the depletion of fossil fuel. also, the pressure of transportation has affected the greenhouse effect and environmental degradation [1]. This energy problem has motivated many researchers to look at alternative energy generation solutions that can meet global energy demand in the long term. Biomass has attracted worldwide attention as a renewable energy source since it can be converted to bio-oil through pyrolysis and has some advantages over fossil fuel. Catalytic pyrolysis of biomass is a promising technique to convert a variety of biomass including sunflower husk, pine wood, rice husk, sugarcane bagasse, palm shell, coconut shell, corn cob and others into many derivative compounds. Catalytic pyrolysis is a thermal degradation process in a free-oxygen environment in which biomass is combined, heated, and pyrolyzed at a high temperature of 300-800 °C in the presence of a catalyst which produces solid, gases, char), liquid (bio-oil) and gas (incondensable gasses) products. The biomass inert gas will be hydro-oxygenated and catalytically cracked to enhance the H/C ratio and calorific value in bio-oil, hence improving the combustion performance and stability of bio-oil.

Thailand has a lot of potential for sustainable agricultural resources. Thailand has a wide variety of crops that can be used as a source of biomass to produce clean energy. One of the most crucial qualities is the heating value of the available bio-oil. Thailand's total coconut planting area is 1,299,799 rai. Nakhon Pathom province has the highest agricultural productivity of coconuts, it was found that each year the coconut has very high productivity of 652,084,186 tons in 2020 resulting in waste agricultural residues produced from coconut milk factory according to a report

from the Office of Agricultural Economics. Catalyst exhibits exceptional activity in the cracking and deoxygenation processes in bio-oil, leading to an increase in hydrocarbon yield and a decrease in oxygenated compounds such as ketone, aldehyde, acid, phenols, and other compounds, which allows it to be converted into good-quality (high aromatic hydrocarbon) bio-oil fuel and expensive-value-added chemicals. Alumina-silica catalyst has been widely utilized widely for bio-oil upgrading [2]. However, the disadvantages are rapid deactivation, excess acidity, which increases viscosity and flash point of bio-oil, and pore size limitation, which prevents large bio-oil components from accessing or dispersing to active sites. As a result, mesoporous activated carbon is an excellent candidate for addressing this issue. The structure and phases of activated carbon are very porous that absorbing metals and metal oxides as a catalyst resulting in the conducive of higher yield of hydrocarbon, H₂, CO gases in pyrolysis product [3]. The transition metals (Ni, Fe, Cu, Pt, etc.) was doped on activated carbon support to improve catalytic deoxygenation performance [4]. The use of transition metal catalysts will increase bio-oil production while additionally affecting chemical compositions. Qiu, B., et al [3] has studied the effect of different transition metals on the bio-oil obtained from catalytic pyrolysis of biomass, the results show that the content of carboxylic acid and oxygenated compounds in bio-oil has decreased and converted into hydrocarbon compounds.

The mentioned issue has encouraged researchers to develop stable, cheap, and environmentally friendly catalysts and the production of high valued-added bio-oil from coconut shell wasted from coconut milk plant. In this study, the impregnation approach was used to synthesize a Ni-doped activated carbon catalyst. The optimal conditions for biomass catalytic pyrolysis were found at three different pyrolysis temperatures (300, 400, and 500 °C). The physical and chemical characteristics of the catalyst were investigated to verify the catalytic results. The product distributions and chemical compositions of the obtained bio-oil were investigated after biomass pyrolysis with/without a synthesized catalyst.

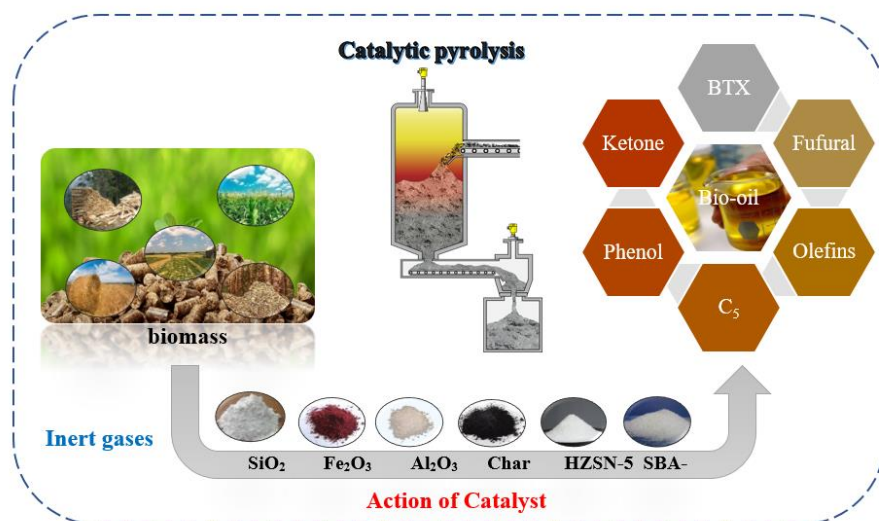


Figure 1 Diagram of catalytic pyrolysis of biomass for producing high-quality liquid fuels and chemicals using various catalysts.

1.2 The objectives of Research

- To produce aromatic-rich bio-oil via catalytic pyrolysis of coconut shell using Ni-doped activated carbon catalyst

1.3 Scopes of Research

- The wasted coconut shell collected from coconut milk plant were pyrolyzed in a fix bed reactor at 400 °C for 2 hr., operating under N₂ gas flow, using furnace as a heating source and Ni-doped activated carbon catalyst.
- Varying Ni loading amount of 0, 5, 10, 15, and 20 wt.% on activated carbon.
- The prepared catalysts were analyzed by XRF, XRD, and BET.

1.4 Experimental locations

- Department of Chemical Engineering, Faculty of Engineering and Industrial Technology, Silpakorn University, Nakhon Pathom 73000, Thailand.
- Chemistry Program, Faculty of Science and Technology, Nakhon Pathom Rajabhat University, Nakhon Pathom 73000, Thailand.

Chapter 2

Literature Reviews

2.1 Biomass

Biomass is an organic material that can be used to produce energy such as agricultural waste (rice straw, sugarcane, tree bark, coconut shells, etc.). Therefore, biomass energy is a type of renewable energy because it is a compound made of carbon and oxygen and made of carbon dioxide and water as well. Photosynthesis is the process of creating energy and nutrients in plants. Most of the biomass is solid. But shape, size and moisture content will differ depending on the type of biomass. Biomass is composed of cellulose, hemicellulose and lignin, whose structure is mainly composed of sugars and polymers called polysaccharides.

Cellulose is a polysaccharide fiber that is the main component of plant cell walls and is the most naturally occurring organic substance. Cellulose is mostly found in wood. The main chemical property of cellulose is that it is insoluble and inert, especially in hydrolysis reaction. Hemicellulose co-occurs with cellulose but is an amorphous form with a different chemical atomic arrangement and low mass. Most cellulose is formed from a simple sugar molecule called D-glucose. Hemicellulose, on the other hand, is made up of many different monosaccharides joined together in a branch rather than a straight line. Lignin is composed of the aromatic structure of phenol, propane, connected as aliphatic chain and is amorphous form as hemicellulose. High lignin biomass favor coke production and less aromatic yield While high hemicellulose favor high non-condensable gases and low coke production. The biomass with low lignin and high cellulose/hemicellulose favor for activated carbon production. Many agricultural residues such as pine wood contain cellulose 48%, hemicellulose 10 %, and lignin 24 %. Rice husks contain cellulose 28%, hemicellulose 26%, and lignin 27%. Eucalyptus contains cellulose 44%, hemicellulose 24%, and lignin 28%. The major components of biomass are shown in Fig 2 [5].

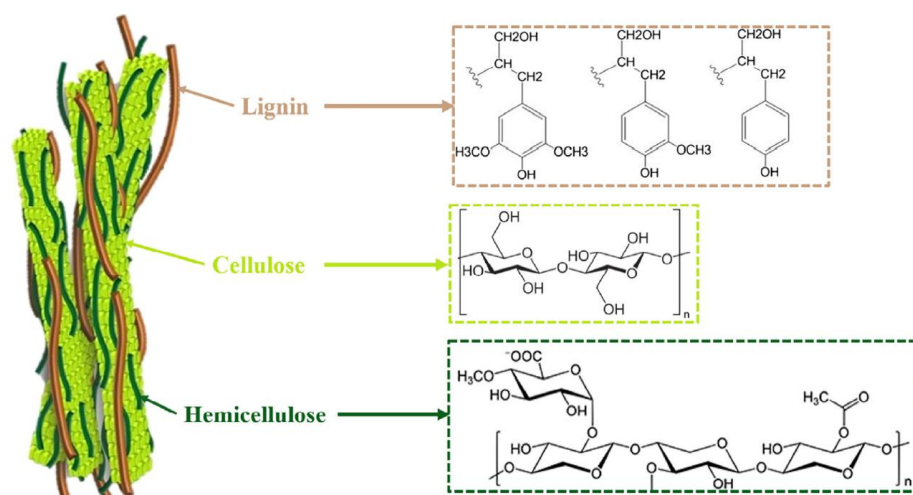


Figure 2 The major components of biomass [6].

2.2 Coconut shell

Coconut is an important plant in Thailand's economy. Coconut is a perennial plant. Characteristics of feather-like compound leaves. It consists of an outer shell, coconut fiber and coconut shell. Coconut is the main agricultural product of Nakhon Pathom Province as shown in Fig 3. It was found that each year the coconut has very high productivity resulting in waste agricultural residues produced from coconut milk factory. One coconut consists of 20% coconut shell, 35% fibers, 25% coconut meat and 20% coconut oil. Coconut shell contains the highest lignin composition of 29-54% followed by coconut fiber (lignin 33-53%), leaves (lignin 33-45%), husk (lignin 25-42%) and frond (lignin 18-21%) [7]. With these properties of coconut and high coconut wasted residues quantity, coconut has potential to be converted into high-value product such as bio-oil and reduce wasted coconut in Nakhon Pathom.

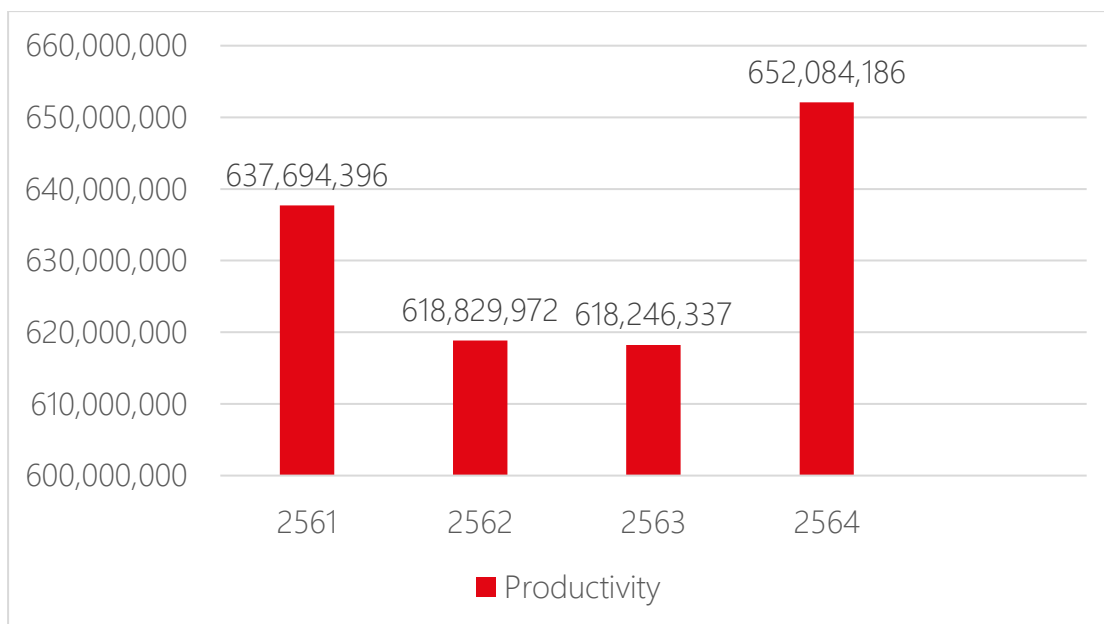


Figure 3 The coconut productivity of Nakhon Pathom.

2.3 Pyrolysis process

Pyrolysis is the breakdown of biomass with heat under an oxygen-free atmosphere and irreversible reaction. Biomass is decomposed and converted into products. Initial products have both stable and unstable parts that can decompose further into the next product. At the end of the reaction or with rapid cooling, the obtained final products are gases, liquids and solids as shown in Fig 4.

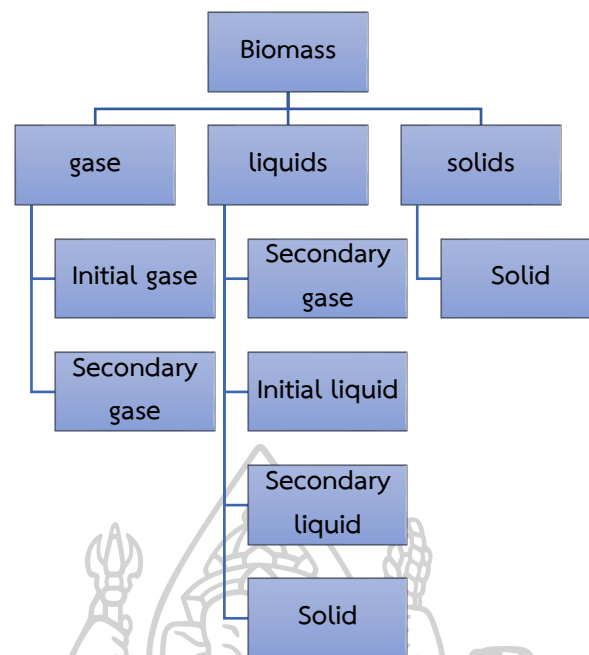


Figure 4 Thermal decomposition process of biomass.

The obtained solid is called charcoal which is mainly composed of carbon material and some inorganic ash. The liquid condensed at room temperature is called pyroligneous liquid or pyroligneous acids or pyrolysis oil. The appearance of the liquid is brown and black which is like crude oil. The pyrolysis process can be controlled to produce the most product at any state by controlling various factors such as heating rate, temperature, reaction time and so on (Nakorn Tippayawong, Biomass Conversion Technology, pp. 268-269).

The physicochemical processes that occur during pyrolysis (Ramanathan et al, 2022, [8]) are as follows.

1. The heat source provides heat transfer to the biomass to increase the temperature inside the biomass.
2. Initial pyrolysis reaction releases volatile vapors and produces charcoal.
3. The flow of hot volatile vapors through the biomass causes heat transfer between volatile vapors and biomass.

4. Condensation of large-molecule volatile vapors inside the biomass followed by secondary pyrolysis reaction can convert initial volatile vapors into crude oil.
5. In the self-catalyzed secondary reaction along with the primary pyrolysis cause a competition for the reactants in the reaction.
6. When thermal decomposition has increased, there are co-reactions occurred such as gas reforming reactions, the conversion of solid molecules into gas with water, radical aggregation reaction, dehydration which depends on residence time, temperature, and pressure.

2.4 Type of pyrolysis process

Pyrolysis is a thermochemical mechanism that converts biomass and polymers into high-energy fuel. Biochar, bio-oil, and gas are produced by heating at medium temperature of 500-800 °C in a free-oxygen environment. The amount of product from the pyrolysis process depends on several factors.

2.4.1 Slow pyrolysis

Slow pyrolysis occurs when the reaction temperature ranges between 400-600 °C with a low heating rate (less than 10°C/minute). The diameter of the feedstock is more than 2 mm. Slow pyrolysis products are liquid 30-50% and biochar 25-35%. Slow Pyrolysis can also be classified into two types (carbonization and conventional pyrolysis) [9]. Carbonization pyrolysis is a long-term heating process that takes about a day to produce charcoal as cooking fuel and the gaseous product released into the atmosphere. Conventional pyrolysis is a process that takes less than 15-30 minutes to produce the product in all three states: charcoal, oil, and non-condensable gas. The slow pyrolysis provides a small amount of oil product [10]. Therefore, most bio-oil is used as fuel in the combustion process. However, the water-soluble parts of the bio-oil can be separated by utilizing some chemicals (acetone, ketone, methanol, formic acid, acetic acid, etc.) that can extract the water-soluble parts from bio-oil [11, 12].

RV, Rubi. et al [13] has studied slow pyrolysis of buri palm to investigate the effect of pyrolysis temperature and residence time. The buri palm pyrolysis was performed in a fixed bed reactor with different pyrolysis temperatures of 300, 500 and 700 °C and residence time of 30, 60 and 90 mins. The optimized condition for the highest biochar content was 300 °C temperature and 90 mins residence time. While the highest bio-oil content of 46% obtained from 500 °C temperature and 90 mins. It was found that the biochar content increases with the increasing of residence time but decreases with the increasing of temperature. The HHV of biochar at 300 °C, 30 mins was 16.93 KJ/kg and HHV of biochar at 700 °C, 30 mins was 28 MJ/kg.

S, Modak. et al [14] has studied slow pyrolysis of cooked food waste at pyrolysis temperature of 300, 400 and 500 °C to produce bio-oil. The chemical composition of bio-oil obtained at 300 °C was mainly composed of carbonyl compounds, furans and Levoglucosan. While bio-oil obtained at 400 °C is composed of different compounds such as aliphatic compounds, phenolic compounds, alcohol, acid, and nitrogen compounds. The bio-oil obtained at 500 °C is composed of aromatic compounds up to 60 %.

2.4.2 Fast pyrolysis

Fast Pyrolysis is bio-oil-producing process, the reaction temperature between 400 - 650 °C with a high heating rate (>1000 °C/secs), less feedstock diameter of <2 mm, short residence time of the vapor in the reactor (< 2 secs) [15]. There are more than 3,000 types of compounds found in bio-oil. In fast pyrolysis of biomass, the obtained product is composed of liquid 60-75%, solid 15-25%, non-condensable gas 10-15%, and water content 10-30% depending on the moisture content contained in the initial biomass. There are various compounds in bio-oil which obtained by thermal decomposition of cellulose, hemicellulose, and lignin [16]. Most of the chemical composition of bio-oil from biomass is shown in Table 1. However, due to most of the chemical compound in bio-oil is organic compounds, so bio-oil produced from the fast pyrolysis can be further refined into many fuels and chemicals [17].

Table 1 Some chemicals found in bio-oils [18].

Cellulose/Hemicellulose derived Compound	Lignin-derived Compound	Common derivatives
Levoglucosan	Isoeugenol	Char
Hydroxyacetaldehyde	Phenol	Water
Acetic acid	4-ethyl phenol	CO, CO ₂ , CH ₄ , C ₂ H ₆
Acetol	2-ethyl phenol	
Furfural	p-cresol	
Furfuryl alcohol	o-cresol	
Cellobiose	m-cresol	
2-methyl-2-cyclopenten-1-one	2,6-dimethoxyphenol	
3-methyl-2-cyclopenten-1-one		

Fast pyrolysis consists of four important steps: (1) due to fast pyrolysis is high heating and heat transfer rates, so small size of feedstock is required. (2) The precise temperature control of the pyrolysis process is 400-500 °C. (3) short residence time of volatile vapor in reactor should be 2 seconds to avoid secondary reaction of volatile. (4) volatile vapors must be rapidly cooled and condensed to produce bio-crude oil (Nakorn Tippayawong, Biomass Conversion Technology, pp. 268-269). The removal of charcoal and ash must be designed to minimize the charcoal and ash from the product. To get a free-ash product, the oil production process of fast pyrolysis requires a fast pyrolysis reactor, biomass drying, grinding, char removal, oil condensation, and product collection unit, as seen in Fig 5.

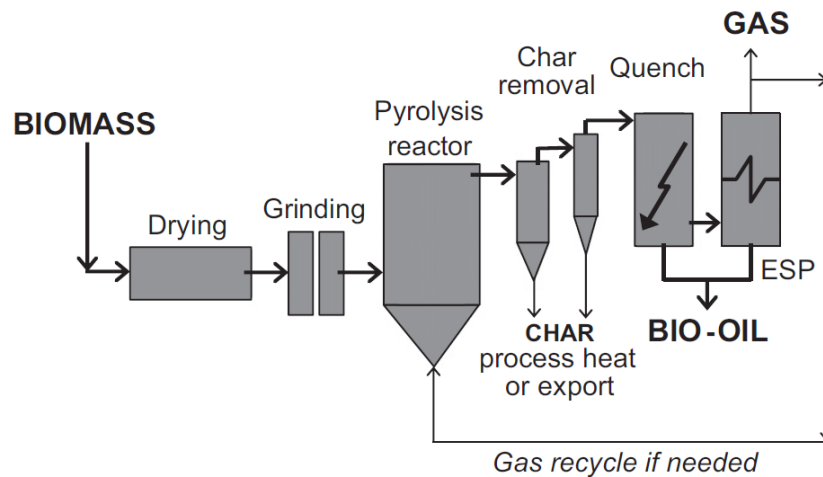


Figure 5 Fast pyrolysis process [19].

N, Abdullah. et al [10] has studied fast and slow pyrolysis of banana at various temperature to produce banana biochar. The fast pyrolysis was carried out in fluidized bed reactor. While fixed bed reactor was used for slow pyrolysis. The result shows that the chemical reactions occurred in fast pyrolysis takes place within 2-2.5 secs. At 500 °C the highest biochar content of 40% was found in fast pyrolysis, while the slow pyrolysis produces the biochar content of 35%. The properties of biochar derived at 500 °C was studied. The result shows that the moisture content and ash content of fast pyrolysis is higher than that of slow pyrolysis. The elemental analysis has shown that slow pyrolysis has higher carbon content, oxygen content, surface area and heating value.

C, Mendoza-Martinez. et al [20] has studied the oxidative fast pyrolysis of eucalyptus wood residues in fluidized reactor. The feed rate was 15.06 kg/h. 480 °C pyrolysis temperature. The product produces gases, bio-oil, and biochar. The gases produced in this process were used as fluidization air energy. The bio-oil obtained 30% yield and 21.4 MJ/kg which indicates that the obtained bio-oil has a good potential for fuel application.

A, Alcazar-Ruiz. et al [21] has studied fast pyrolysis of olive pomace in a Pyroprobe pyrolyzer to produce bio-phenolic compounds under conditions: temperature of 500 °C, heating rate of 20 °C/mins and residence time of 15 secs. Before the pyrolysis process, the feedstock was pretreated by water, acid, and alkali solutions to avoid inorganic elements produced in phenolic product. The result shows that the potassium content is removed and guaiacol produced for water pretreatment. Acid and phenolic compounds have been produced for HCl and HNO₃ solution pretreatment. The sodium content increased to 83% for NaOH pretreatment. The phenolic compound was achieved 36.9% for alkali pretreatment which includes guaiacol 5.9% and vinyl guaiacol 6.2%. This study has proposed an effective pathway to produce bio-phenolic compounds from agricultural residues.

2.5 Pyrolysis of Biomass composition

The chemical composition of biomass is different from that of coal and crude oil. Due to biomass compose of oxygenated compounds so the product produced from biomass pyrolysis is different from fossil fuels. Wood and other biomasses are oxygen-based organic polymer materials such as hemicellulose, cellulose, and lignin. When these compositions are heated, they are thermally decomposed by different pathways and produce a variety of products. To understand the pyrolysis process of biomass Therefore, we must consider the pyrolysis of each major compositions.

2.5.1 Cellulose pyrolysis

The pyrolysis reaction of cellulose is endothermic reaction, and it was found that when cellulose is heated up to 250 °C there is a decrease in the degree of polymerization. The pyrolysis process takes place slowly and yields H₂O, CO₂, CO, and sludge as products. At temperatures above 250 °C, cellulose begins thermally decomposing faster and produce crude -oil, gases, and charcoal. Cellulose decomposition at 240-350 °C produces anhydrocellulose and levoglucosan at 350 °C. The pyrolysis of cellulose takes place even more rapidly above 500 °C, the released volatile vapors are thermally decomposed into gas phase. Q, Lu. et al [22] has

studied the cellulose fast pyrolysis. The study demonstrates the obtained bio-oil composed of water, anhydrosugar, oxygenated compounds and furan derivatives. Cellulose pyrolysis favors the formation of levoglucosan. H, Yang et al [23] has studied catalytic pyrolysis of cellulose for levoglucosenone (LGO) production. The LGO content has increase then decrease in temperature range of 300-500 °C. the maximum LGO content of 46.4% achieved at 400 °C the decrease to 2.48 % at 500 °C. the LGO content has increased as the increasing of catalyst and then LGO decrease at the excess catalyst amount. The optimized condition for LGO production is 400 °C pyrolysis temperature and 1:1 catalyst: cellulose ratio. S, Hameed. et al [24] has studied the product distribution of cellulose pyrolysis in fixed bed reactor. At higher activation energy, the char and tar increase while the gas yield decreases. The distributed activation energy model presents the tar yield of 82.1 wt.%, gas yield of 8 wt.% and char yield of 9.9 wt.%.

2.5.2 Hemicellulose pyrolysis

Hemicellulose pyrolysis reaction is an exothermic reaction and composed of different anhydrous sugars. Hemicellulose has poor polymerization level leading poor resistance to mechanical and chemical decomposition [6]. Pyrolysis of hemicellulose occurs at lower temperatures in the range of 200-260 °C and can occur at wide temperature range. The obtained products are charcoal and bio-oil which less than obtain from cellulose. Most of the hemicellulose does not decompose to the levoglucosan group. The acetic acid produced during the pyrolysis of the biomass contributes to the reduction of the acetyl group (deacetylation) of hemicellulose. In case of the slow pyrolysis of wood, Hemicellulose decomposition occurs before 130-194 °C, but mostly at 180°C. C, Sun. et al [25] has studied the pyrolysis of hemicellulose, cellulose and lignin from wood residues to produce bio-oil. The result shows that the coke produced by hemicellulose pyrolysis while the benzene-ring compounds in the obtained bio-oil was found in cellulose and lignin pyrolysis. The

study demonstrated that high-quality bio-oil can be achieved by removing hemicellulose part from the biomass.

2.5.3 Lignin pyrolysis

properties of lignin depend on the method of lignin extraction. Lignin is the most stable component of biomass and composed of phenolic groups. Lignin is not carbohydrates like hemicellulose and cellulose. At a wide decomposition temperature range (160-900 °C), the pyrolysis of lignin is an exothermic reaction. Below 200°C, the thermal decomposition rate of lignin is very slow. The decomposition of lignin will be more obvious at temperatures between 280 °C and 500 °C. At the highest decomposition rates occurring at 350-450 °C, the decomposition of lignin produces phenolic compounds and more charcoal than cellulose. At a low heating rate, more than 50% of the lignin char is produced by the initial mass. HC, Genuino et al [26] has studied the pyrolysis of lignin to insight into oil yield at various condition: pyrolysis temperature of 250-450 °C, reaction time of 10-50 min, nitrogen gas flow rate 10-30 mL/min. the highest bio-oil yield was 47.1 wt.% at 450 °C temperature and 10 min reaction time. The presence of molten salt in lignin pyrolysis has effectively supported the formation of aromatic and phenolic compounds. S, Sangthon. et al [27] has studied the phenolic-rich bio-oil derived from pyrolysis of palm kernel shell and its isolated lignin in a fixed bed reactor. The bio-oil yield of isolated lignin pyrolysis is higher than that of palm kernel shell pyrolysis. and phenolic production of isolated lignin is more than twice that of palm kernel shell. The phenolic compounds in lignin derived bio-oil are 78% higher than palm kernel shell-derived bio-oil.

2.6 Pyrolysis reactor

2.6.1 Ablative reactor

As shown in Fig 6. A rotating blade (6.35 mm size) is used to press the biomass onto the heated surface with high pressure and temperature of $< 600\text{ }^{\circ}\text{C}$. The rotating blades rotate at about 200 rpm with a relative speed of $> 1.2\text{ m/s}$. The mechanical force from the rotating blade pressed biomass onto the heated surface cause rapid pyrolysis. The released vapors are carried out by nitrogen gas. Charcoal is collected by a cyclone. The reactor has a feed rate of 3 kg of biomass per hour and produces bio-crude oil up to 80% by mass of the initial biomass [28].

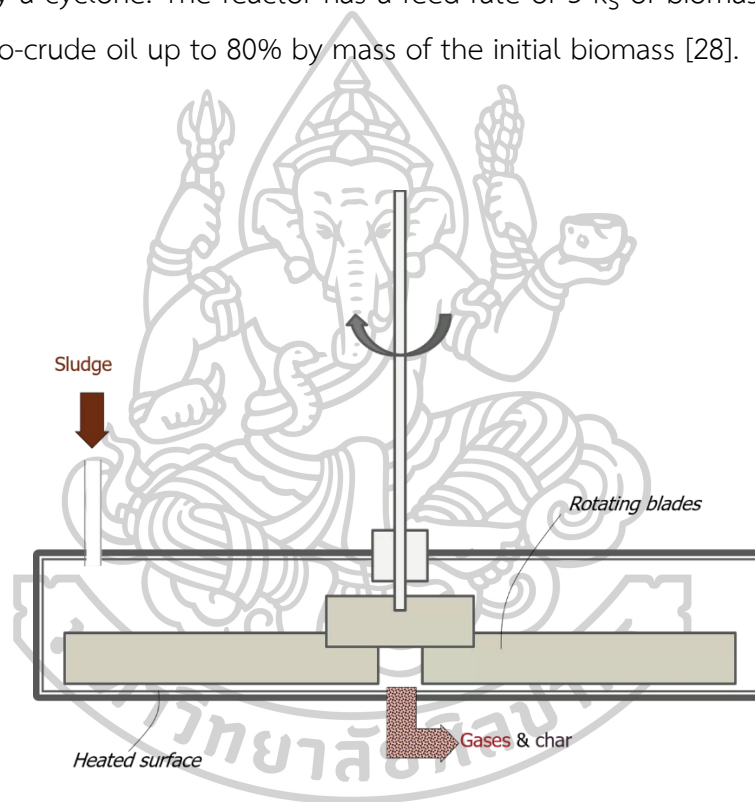


Figure 6 Ablative reactor.

2.6.2 Rotating cone reactor

As shown in Fig 7, A rotating cone pyrolysis reactor is a reactor used in pyrolysis. It is characterized by the process of decomposing materials using heat and high temperature. The rotating cone pyrolysis reactor is characterized by a process that uses the principle of rotation to allow the material to move by gravity, and moves according to the centrifugal force where the material is decomposed as the reactor rotates.

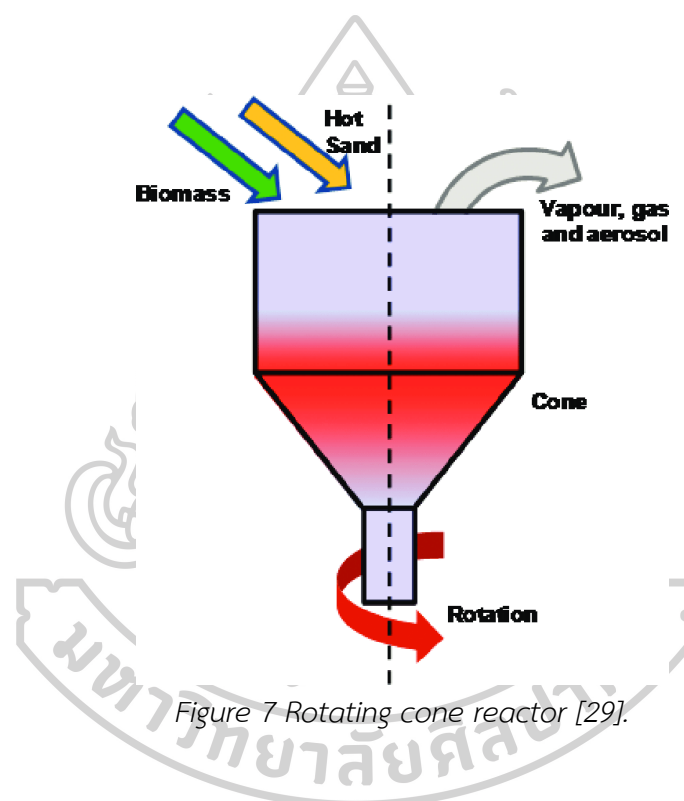


Figure 7 Rotating cone reactor [29].

2.6.3 Fluidized bed reactor

As shown in Fig 8, fluidizing gas is used to create a fluid layer and runs through the distributor plate then lifts the material to become a fluid layer. Fluidizing gas and hot bed particles transfer heat to biomass, resulting in pyrolysis reaction. Volatile vapors and charcoal are released to the top and separated in the cyclone and the condenser to be product [30]. The solid substrate in a fluidized bed reactor is usually supported by a porous plate called a carrier. The liquid is then forced through the distributor through the solid material. At lower fluid velocities, solids remain stationary as the fluid passes through gaps in the material. This is known as a bed

reactor. As the velocity of the fluid increases, the reactor reaches a stage where the force of the fluid on the solid is sufficient to balance the weight of the solid. This step is called incipient fluidization and occurs at the minimum fluidization velocity. When this minimum speed is exceeded, the contents of the reactor bed begin to expand and spin around like a turbulent tank or boiler. The reactor is now a fluidized bed type. Depending on the operating conditions and properties of the solid phase, various flow systems can be observed in this reactor.

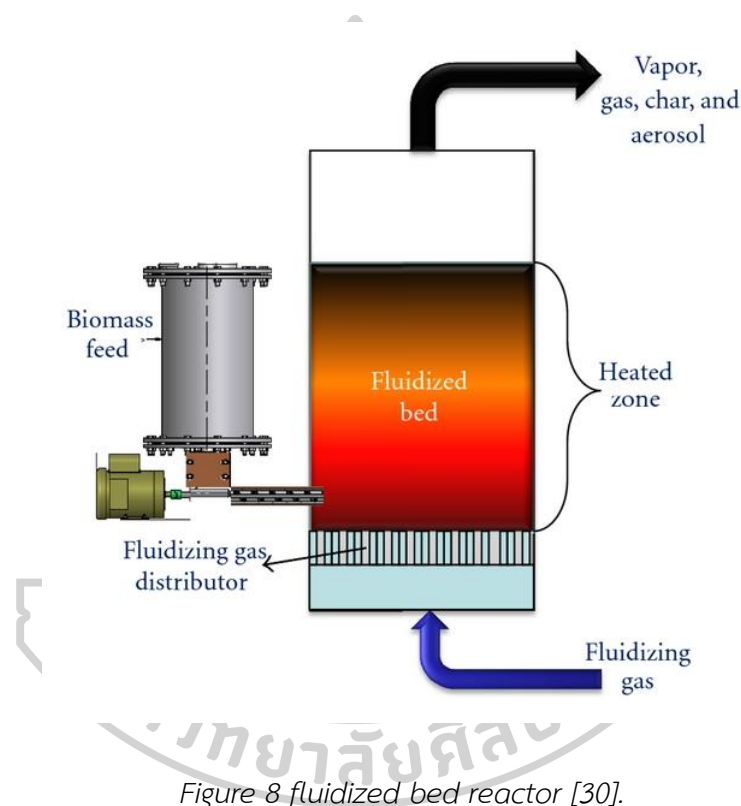


Figure 8. fluidized bed reactor [30].

2.6.4 Circulating fluid bed reactor

The pyrolysis reactor is composed of two parts, The first part is a combustion chamber located at the bottom for heating the sand grains. The second part is a fluid layer, and the biomass feeding ports are located at the top, as shown in Fig 9. The biomass mixed with hot sand undergoes pyrolysis reactions. The hot gases carry volatile vapors, chars, and sand out of the top and into the cyclone. A vortex of swirling air in the cyclone separates char and sand out and cycles back to the

combustion chamber to combust charcoal and sand. Vapors are separated and condensed to produce bio-oil. This reactor consumes 10 kg of biomass per hour and yields 61% of bio-oil by mass of the initial biomass. R Suntivarakorn et al [31] has studied Napier grass pyrolysis in circulating fluidized bed reactor. It was found that the maximum bio-oil was 32.97 wt.% at bed temperature of 480 °C, superficial velocity of 7 m/s and feed rate of 60 kg/hr. while the predicted value of bio-oil was 32.97 wt.%. The obtained bio-oil has water content of 48.15 wt.%, heating value of 19.79 MJ/kg, density of 1,274 kg/m and viscosity of 2.32 cSt.

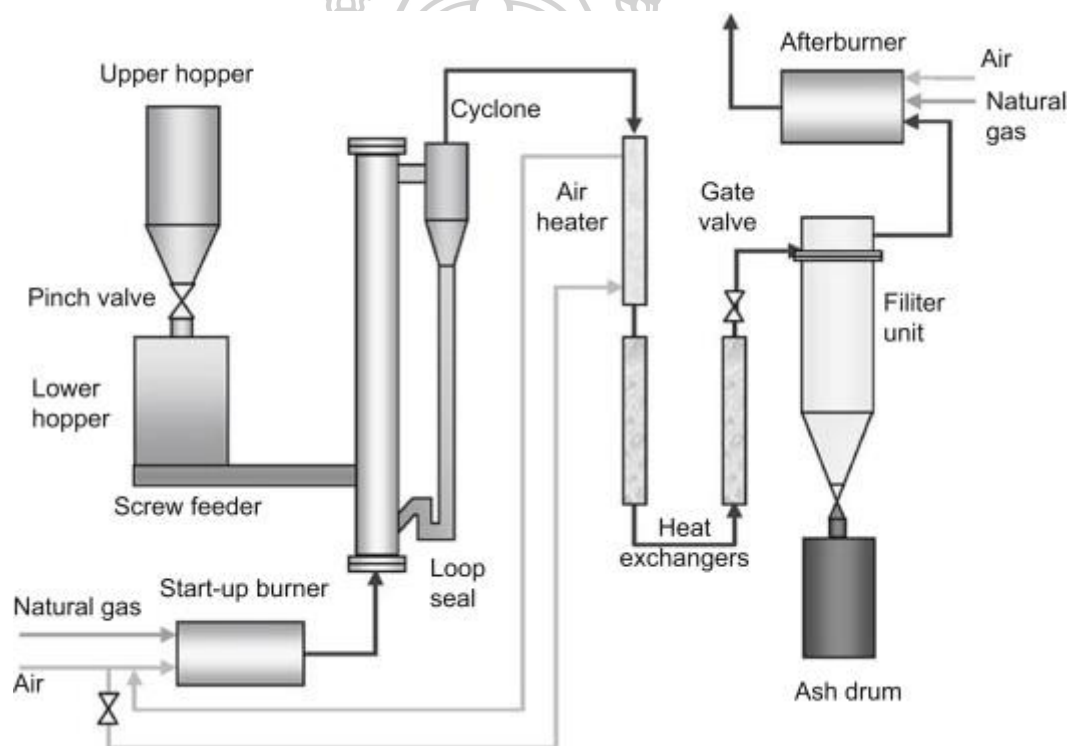


Figure 9 Circulating fluids bed reactor [32].

2.6.5 Entrained flow reactor

As seen in Fig 10. The milled biomass has a particle size of roughly 1.5 mm. The heat source is generated by the combustion of propane gas and air, which produces hot gas of 927 °C. This hot gas interacts with and transports the biomass in the furnace chamber, resulting in fast pyrolysis. This reactor has a feed rate of 57 kg/hr. The maximum bio-oil production is 60%. Entrained flow reactors are used for fundamental combustion investigations of solid fuels under exactly defined conditions. They are also used in experimental carbonation of CaO [33] and as an entrained flow gasifier model for process development [34]. K Maliutina et al [35] has studied pyrolysis of microalgae (MA) and palm kernel shell (PKS) in entrained-flow reactor in temperature range of 600-900 °C. it was found that the highest MA-derived bio-oil was 60.22 wt.% at 800 °C and the highest PKS-derived bio-oil was 73.74 wt.% at 600 °C. MA-derived bio-oil comprised a high hydrocarbons and nitrogen-containing compounds, while PKS-derived bio-oil was mostly composed of phenols, esters, and hydrocarbons.

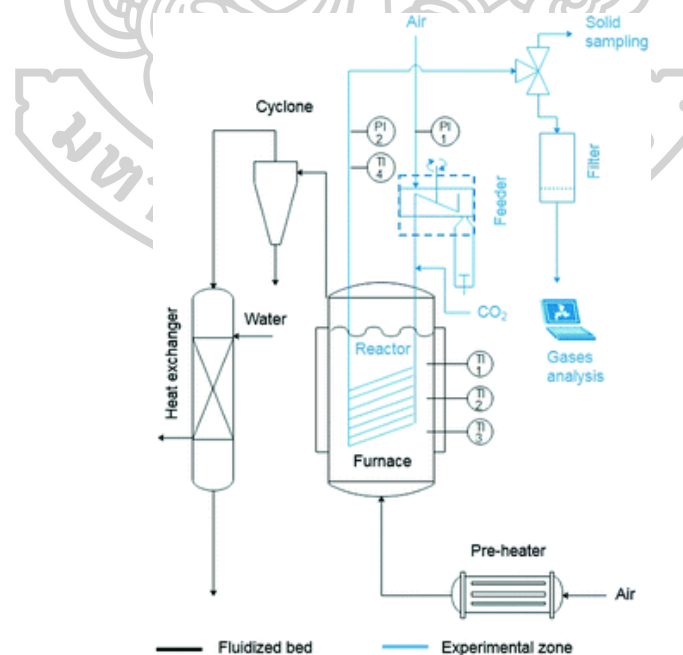


Figure 10 Entrained flow reactor [33].

2.6.6 Vacuum moving bed reactor

Operating under a vacuum reduces the residence time of the pyrolysis vapors, thereby limiting secondary vapor reactions and increasing the yield of bio-oil [36]. Reactor used in vacuum pyrolysis process with loss of oxygen and carbon. and changes in various substances in the materials used. The chopped and dried biomass is fed from above and placed on a support plate within the oven. The biomass will be pushed along the rail gradually and heated by molten salt at 530°C. The molten salt will return and receive heat from uncondensed gas combustion, which then transfers the heat to the furnace as shown in Fig 11. This reactor can produce roughly 65% bio-oil and 25% charcoal.

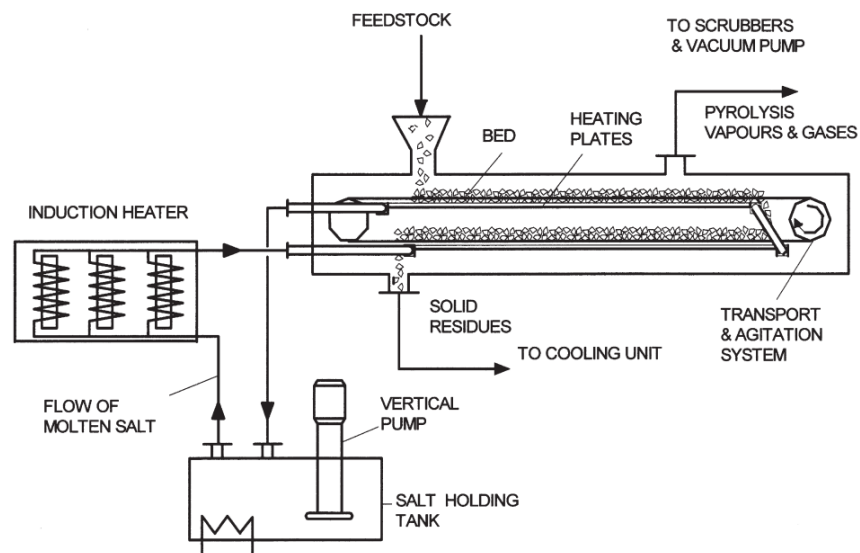


Figure 11. The vacuum moving bed reactor [37].

Table 2. summarizes the advantages and disadvantages of each type of pyrolysis reactor. Choosing the right reactor to obtain the desired product is very important. However, the appropriate conditions for operating the pyrolysis reactor must be taken into account in order to reduce production costs and time.

A variety of techniques are available for improving biomass via thermochemical conversion. Table 3 shows the key differences between these technologies. This study has reported interesting processes including fast pyrolysis, slow pyrolysis, and torrefaction as follows.

Table 2 The reactor type, bio-oil production, and applications.

Reactor type	Reaction rate	Bio-oil yield (wt.%)	Inert gas requirement	Residence time	Advantages	Disadvantages	Production level	Operational status
Fixed bed	Slow pyrolysis	36-49 (According to this work)	Low	High	Most cost-effective in converting biomass into fuels; Deactivated catalyst is easily removed. and replaced; Deactivated catalyst is easily recycled & purified; Compatible with any Cat & solvents; Commercially available.	Pressure drop across the bed can be problematic; Poorer mixing can reduce the selectivity and produce hotspots within the reactor.	Large scale	Commercial
					Accommodate large size of biomass			

Reactor type	Reaction rate	Bio-oil yield (wt.%)	Inert gas requirement	Residence time	Advantages	Disadvantages	Production level	Operational status
Fluidized bed	Fast pyrolysis	75	High	Low	High heat and mass transfer; Economical operation; Commercial potential.	Non-uniform residence time of solids. Difficult to separate solid products. Only accommodate with small biomass particles	Medium scale	Commercial
Spouted bed	Fast pyrolysis	70	High	Low	Accommodate large size of biomass	Design is complex; it is not cost effective.	Medium scale	Laboratory
Rotating cone	Fast pyrolysis	60-70	Low	Low	Economical in operation	Difficult to scaling up due to design constrains.	Medium scale	Commercial
Auger reactors	Slow and fast pyrolysis	42-74	Low	High and low	Commercially potential	High biochar production	Small scale	Demonstration
Ablative	Fast pyrolysis	65	Low	Low	Commercially potential.	Heat transfer is not uniform.	Small scale	Laboratory

Table 3 Processes for the thermochemical conversion of biomass.

Technology	Temperature	Heating rate	Pressure	Reaction time	Medium	Target product
Torrefaction [38]	200-350 °C	-	Atmospheric	15-45 min	50 mL/min of CO ₂ gas.	Torrefied biomass
Slow pyrolysis [10]	400 °C	10 °C/min.	Atmospheric	Hours	0.5 L/min of N ₂	Biochar
Fast pyrolysis [39]	550-700 °C	> 1000 °C/min	Atmospheric or vacuum	30 min	100 mL/min of N ₂ gas	Fuel
Flash carbonization [40]	400 °C	-	30 MPa	-	Oxygen-free atmosphere/air	Char
Gasification [41]	800-900 °C	-	-	> 30 min	200 and 400mL/min of N ₂ gas	Gas
Wet torrefaction [42]	220 °C	-	Water saturation pressure	5 min	Water	Hydrochar
Hydrothermal liquefaction [11]	300 °C	2 °C/min	10.2 MP	1.9 hr	Water	Liquid product

Technology	Temperature	Heating rate	Pressure	Reaction time	Medium	Target product
Supercritical water Gasification [43]	450 °C	-	10 mL/min reaction	-	Supercritical water	Gas
Plasma pyrolysis [44]	1200 watt	-	9 SLM	5 min	Ionized gas	Gas



2.7 Catalyst

The catalyst used in the pyrolysis process is the catalyst of transition metals which are prepared in solid form. The components of the catalyst can be divided into 3 parts according to their functions including active agent, support, and promoter. In the catalyst industry used mainly metal-based catalysts. This type of catalyst has advantages: Safe and easy to procure and prepare, Compatible with many reactors, Metal particles are separated independently. When performed at high temperature, the metal particles are not combined into large particles, and this type of catalyst, the support can also be a promoter. Alumina-silica catalyst has been widely used for bio-oil upgrading but the disadvantage of this catalyst is rapid deactivation, excess acidity which increase viscosity and flash point of bio-oil, pore size is limitation which prevent large component of bio-oil from accessing or dispersing to active sites. To solve this problem the mesoporous activated carbon was used in this work. The advantage of activated carbon is highly porous and has phase that can absorb transition metal for enhancing yield of product. Transition metal (Ni, Fe, Cu Pt etc.) was doped in activated carbon support to improve catalytic activity and improve bio-oil yield and chemical composition [45]. And the detailed development of these catalysts was as follows.

2.7.1 Microporous zeolite

Microporous zeolite catalysts are a type of catalyst that have micropores in the catalyst structure. Microporous molecule sieves such as ZSM-5, HY, USY, H-ferrierite, H-Mordenite etc. ZSM-5 has uniform pore and pore size, making it appropriate for shape selectivity catalysis and aromatic and olefin production. ZSM-5 reduces the acid and alcohol content of bio-oil while increasing the ketone content [3]. S Dong et al [46] has studied ZSM-5 used in catalytic conversion of plastic pyrolysis oil. The result shows that 1-Octene degrades into smaller olefins, which undergo further cracking, oligomerization, cyclisation, and hydrogen transfer to produce benzene, toluene, xylene (BTX), coke, and hydrogen.

The addition of metal on HZSM-5 catalyst shows the different effect on yield and selectivity of bio-aromatic due to the increase of acid site and transformation of

Bronsted acid to Lewis acid, which resulting in the reduction of coke and catalyst deactivation. Tshabalala, T.E et al [47] has studied metal (Ga, Mo, Zn)-modified HZSM-5 catalyst on aromatization of n-hexane. Zn and Ga-doped H-ZSM-5 catalysts show high aromatic selectivity. The aromatic yield of Zn and Ga-doped H-ZSM-5 catalysts were 32 %. While the aromatic yield of H-ZSM-5 and Mo-H-ZSM-5 catalysts were 22 and 18 %. Chaihad, N., et al [48] investigated Cu-doped HZSM-5 catalyst in fast pyrolysis of sunflower stalks. A 0.5%Cu/HZSM-5 catalyst produced the highest amount of aromatic hydrocarbon content of 73 % and aromatic selectivity yield up to 56 % which higher than that of HZSM-5 (26 %). Veses, A., et al [49] has studied the effect of metal-modified zeolite catalyst on bio-oil properties. The phenol was converted by metal-catalyst and get through several reactions (de-carbonylation, cracking). The side products produced during several reactions are H₂O, CO, CO₂, and coke. The target product produced in the process is full of aromatic compounds, less oxygen content, less total acidity, and high heating value. Vichaphund, S., et al [50] has studied Co, Ni, Mo, Ga and Pd metal-doped HZSM-5 catalysts in pyrolysis of Jatropha biomass. The metal-doped HZSM-5 catalysts were prepared by two methods which are ion-exchange and impregnation method. Ga and Pd-HZSM-5_{ion-exchange} show the highest aromatic content of 27 % and aliphatic content of 6 %. While Ni/HZSM-5_{ion-exchange} and Ga/HZSM-5_{ion-exchange} show aromatic content of 30.6 % and of 39 %, respectively. So, it can conclude that Ga/HZSM-5 catalyst produced by impregnation method is the best catalyst with phenol content of 5.6 %, acids content of 3.7 %.

2.7.2 Mesoporous zeolite

Metal and metal oxide in mesoporous zeolite has widely considered as an advanced catalyst because of their high-temperature thermal reaction, good photoelectric performance, and high effective conversion of CO₂ to CH₄ [51]. Karnjanakom, S., et al [52] studied Mg-based Al-MCM-41 catalyst in fast pyrolysis of cellulose, lignin, and sunflower stalks. The result shows that the pore volume and pore size decrease with the increasing of Mg concentration. The acidity also decreases with the increasing of Mg loading amount. There are no found dominant

peaks of Mg particle on XRD pattern in any percent loading amount of Mg. This indicates that Mg particle is well dispersed on support. The chemical composition and aromatic selectivity result has shown that the bio-oil is greatly improved when Mg-doped Al-MCM-41 catalyst applied in pyrolysis of all feedstocks. a 1 wt.% Mg/Al-MCM-41 catalyst present 5 times reuse of spent catalyst. Zhao, M., et al [53] investigate Ni-MCM-41 catalysts in the cellulose pyrolysis for product gas distribution and H₂ production. The catalyst particle (Ni) is spread throughout the support of MCM-41, which has a high mesoporous structure. MCM-41 with 5% Ni loading had a consistent distribution of Ni particles that were the same size as the pores in the support. However, at higher Ni loadings, it exhibits a non-uniform particle distribution and a wide particle size range. The distribution of Ni particles on MCM-41 supports has a substantial impact on the catalyst's activity for increasing gas production. The maximum H₂ selectivity, H₂ yield, and total gas production are obtained in 5 wt.%Ni/MCM-41.

2.7.3 Metal oxide catalyst

Metal oxide catalysts are a type of catalyst that contain metal oxides. They are used in many industrial processes such as the production of sulfuric acid, nitric acid, and ammonia. Metal oxide catalysts are also used in the production of biodiesel and biofuel because of high dispersion, good adsorption, and excellent properties in biomass pyrolysis. Main metal oxide catalysts were MgO, Al₂O₃, SiO₂, ZnO, NiO etc. E.F. Iliopoulou [54] investigated the metal oxide catalysts in the catalytic pyrolysis of olive mill wastes. Fe and Mn oxide catalysts, based on alumina, silica and magnesia supports are among metal oxide catalysts. Fe₂O₃ and MnO catalysts exhibit an effective catalysis for retaining organic yield and improving bio-oil quality.

Alumina and silica oxide catalyst are important candidate catalyst due to its high thermal stability and surface area [55] and they exhibit exceptional catalytic performance for acid catalysis. The use of Al₂O₃ and SiO₂ has some disadvantages due to high gas and tar production. Zheng, Y., et al [56] investigated the combination of two oxide (Mo₂N and Al₂O₃) catalyst in fast pyrolysis of lignin for

aromatic hydrocarbon production. The result shows that there are high non-condensable gases produced in the absence of catalyst. The non-condensable gases produced less when $\text{MoO}_3/\text{Al}_2\text{O}_3$ and $\text{Mo}_2\text{N}/\text{Al}_2\text{O}_3$ catalysts applied. The pore volume, size, and surface area of Al_2O_3 decreased with Mo_2N and MoO_3 loading. The aromatic selectivity shows that $\text{Mo}_2\text{N}/\text{Al}_2\text{O}_3$ catalyst produces benzene 45 % and toluene 15 %, while $\text{MoO}_3/\text{Al}_2\text{O}_3$ catalyst produces benzene 5 % and toluene 3 %.

The addition of transition metal on acidic metal oxides improved the thermal stability of the catalyst and increased the number of chemisorbed oxygen and Lewis's acid sites on the surface of the catalyst [57]. Karnjanakom, S., et al [58] has studied metal (Zn, Ce and Ni)-doped alumina catalyst in fast pyrolysis of sunflower stalk for upgrading bio-oil quality. The result shows that the surface area, pore volume and pore size decrease with the increasing of metal loading on Al_2O_3 -0.5. 2.5%Ni- Al_2O_3 -0.5 present the lowest coke decomposition of 5.37%. The XRD pattern has confirmed the presence of metal oxide on Al_2O_3 -0.5 support. The bio-oil yield decreases with the increasing of the catalyst content used in pyrolysis process. The 2.5%Ni- Al_2O_3 -0.5 catalyst shows the best catalytic performance with high aromatic hydrocarbon content of 92% and aromatic selectivity. The activity performance of spent catalyst was recovered at 650 °C of calcination for 30 minutes.

2.7.4 Carbon-based catalyst

The metal carbon-based catalyst prepared by metal supported on activated carbon shows highly porous structure and phase of metals and metals oxides. The metal-based carbon catalyst is conducive to obtain higher yield of hydrocarbon and H_2 and CO gases in pyrolysis product [3]. Maneechakr, P., et al [4] investigated Cu, Ni, or Fe-doped carbon catalyst in palm kernel cake pyrolysis. Waste palm kernel cake used as a biomass feedstock to produce bio-oil fuel and catalysts/supports. The physiochemistry properties of prepared catalyst shown that the surface area, pore volume and pore size decrease with the increasing of Metal loading amount this indicate that the activated carbon surface and pore were occupied by metal

particles. The crystallite size of metal loading on activated carbon was increasing with the metal loading amount. The acidity of prepared catalyst increases with increasing of Metal loading amount. The XRD result shows the dominant peaks of metal on activated carbon. XRD pattern of Ni-doped catalyst has shown the Ni particle around 45, 53 and 78 cm^{-1} . For other metal Cu and Fe show their peak at different wavenumber. The chemical composition of obtained upgraded bio-oil has shown catalytic performance. The result shows that there is aromatic hydrocarbon increase dramatically after using metal-activated carbon catalyst. This indicates that some oxygenated compound in non-upgraded bio-oil has converted into aromatic hydrocarbon. 15% loading amount show that highest aromatic content of all metal (Cu, Ni, Fe). Where the 15% Ni loading has the highest aromatic content compared to Cu and Fe metal.

Activated carbon be synthesized from many resource. Yuan, C., et al [59] has synthesized activated carbon catalyst from seaweed and used the synthesized catalyst in the catalytic pyrolysis of wasted clay oil for biofuel production. The seaweed derived activated carbon were prepared by activation at different temperature 600, 700 and 800 $^{\circ}\text{C}$. The result shows that at 800 $^{\circ}\text{C}$ activation temperature present surface area and average pore size of 1227.74 m^2/g and 3.79 nm, respectively. The Cu metal was then loaded on a seaweed derived activated carbon with Cu concentration of 5, 10, 15, 20 wt.%. The XRD result shows the peaks of Cu component on seaweed derived activated carbon support at 44, 52 and 74 cm^{-1} . The highest heating value (48402 kJ/kg) of biofuel was found in specific condition where biomass: catalyst ratio of 10:1, 15% of Cu loading amount on activated carbon support derived at activation temperature 800 $^{\circ}\text{C}$. at this specific condition has produced liquid yield of 76.31 %, gases yield of 20.26% and solid yield of 3.43 %, aromatic hydrocarbon content of 46 % and chain hydrocarbon content of 45 %. The hydrogen content in gas products is reduced due to hydrogenation reaction. Di Stasi, C., et al [60] synthesized an activated biochar from wheat straw and the activated biochar was doped by Ni and Co metal to investigated the steam reforming of slow pyrolysis oil. The wheat straw-derived biochar shows the potential support catalyst. For the steam reforming of acetic acid, a 10% Ni demonstrated efficient acetic acid

conversion and resistance to deactivation. The addition of a second metal (cobalt 7 wt.%) greatly enhanced catalytic activity and stability. For steam reforming, an activated biochar-supported Ni-Co catalyst was evaluated. The presence of sugar in derived compounds quickly deactivated the bimetallic catalyst, according to the results. In ideal operating conditions, it appears possible to achieve a total carbon conversion of 65% and a hydrogen selectivity of 55%. It concludes that activated biochar can improve the pyrolysis oil. The bimetallic Ni-Co catalyst performs the best in acetic acid reforming. Heavy organic molecules have the potential to damage the catalyst's active sites. The steam reforming of pyrolysis oil demonstrated a carbon conversion of 65%. In the first 850 minutes, the catalyst is not deactivated.

Additionally, activated carbon can also be used as a microwave susceptor in microwave-assisted pyrolysis by using microwave energy as heat energy. The microwave susceptor improves the heating rate, and the heating rate improves the liquid, gas and solid yields [61, 62]. The usage of activated carbon susceptor has improved the yields of bio-oil, biochar, and syngas due to the improvement of heat transfer and residence time which provide fast pyrolysis. Omoriyekomwan, J.E., et al [63] studied activated carbon (AC) as microwave susceptor in microwave pyrolysis of palm kernel shell for the production of phenol-rich bio-oil. The selectivity of phenol rose dramatically in catalytic microwave pyrolysis. When using AC and a pyrolysis temperature of 500 °C under microwave pyrolysis conditions, the result showed a total phenolic concentration of 71.24% and the highest phenol concentration in bio-oil of 64.58%. The enhanced phenol yields were attributed to AC boosting demethylation, decarboxylation, and dehydration processes. The functional groups of OH, C-H, C=O, and C-O reduced during pyrolysis, according to Fourier transform infrared spectroscopy (FTIR) data. Lam, S.S., et al [64] has studied activated carbon susceptor in microwave assisted pyrolysis of wasted palm oil. The pyrolysis temperature was performed in the range of 350-550 °C. It was found that the lowest bio-oil obtained at 350 °C and the highest bio-oil yield of 70% obtained at 450 °C. There are many chemical compounds produced such as alkane, alkene, cycloalkane, carboxylic acid, ketone, aldehyde, and other compounds. Most of the compounds produced in bio-oil were alkane and alkene. The comparative study has studied the

heating value of bio-oil obtained from microwave pyrolysis and biodiesel from transesterification and diesel from transport grade. The heating value of bio-oil from microwave pyrolysis is 46 MJ/kg, the heating value of biodiesel from transesterification is 37-43 MJ/kg and heating value of diesel (transport-grade) is 45 MJ/kg.



Chapter 3

Theory

3.1 Pyrolysis behavior of lignocellulose biomass

Lignocellulosic biomass is composed of 40-60% cellulose which is made up of glucose monomer. The long-chain cellulose polymers require 166-250 kJ/mol of activation energy to breakdown glycosidic bonds in cellulose. The decomposition of cellulose mainly occurs in a temperature range of 315-400 °C. At lower temperature <300 °C, the cellulose will breakdown and produce non-volatile oligosaccharides. At a higher temperature range of 300-400 °C, the cellulose more produces monomeric sugar such as levoglucosenone which is the major composition in bio-oil and many reactions occur in this temperature range such as ring-opening polymerization, dehydration, carbonylation. At higher temperature > 450 °C, the production of furfural-based compounds (furfural and 5-hydromethylfurfural) is observed due to the secondary decomposition of monomeric sugars. The secondary decomposition of monomeric sugars and furfural-based compounds produce low-molecular weight compounds including hydroxyacetaldehyde (HHA) as the final product as shown in Fig 12 [6].

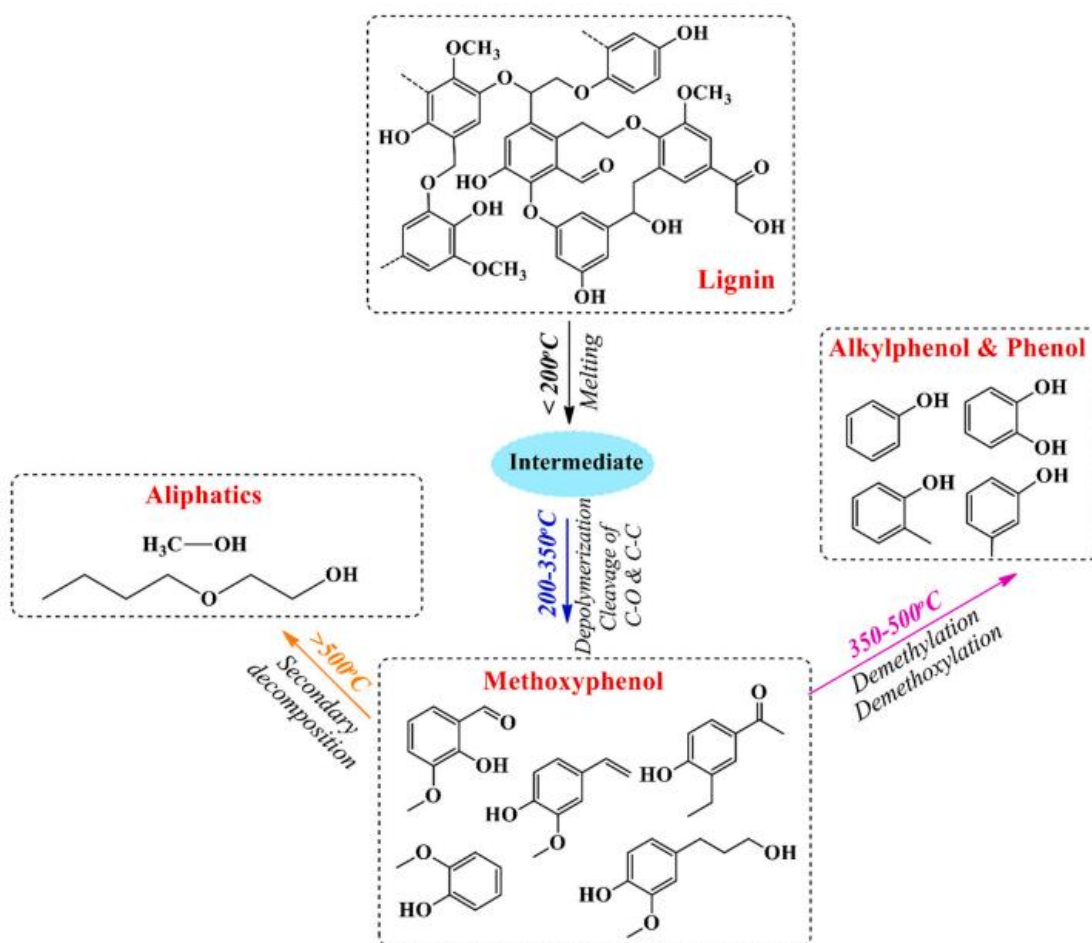


Figure 12 Pyrolysis behavior of cellulose [6].

Lignin is composed of different oxygen-containing functional groups such as carboxyl, carbonyl, hydroxyl and methoxyl groups. The higher content of methoxyl groups in lignin results in the lower production of char. At higher temperature 200-300 °C, the depolymerization of intermedia produce aromatic alcohols then converts them into methoxyphenol. The temperature continues increasing up to 350-500 °C, the alkylphenol and phenol are found in the decomposition of methoxyphenol via demethylation and demethoxylation reactions. Finally, temperature above 500 °C, the secondary decomposition of methoxyphenol produces aliphatic and methanol compounds as shown in Fig 13 [6].

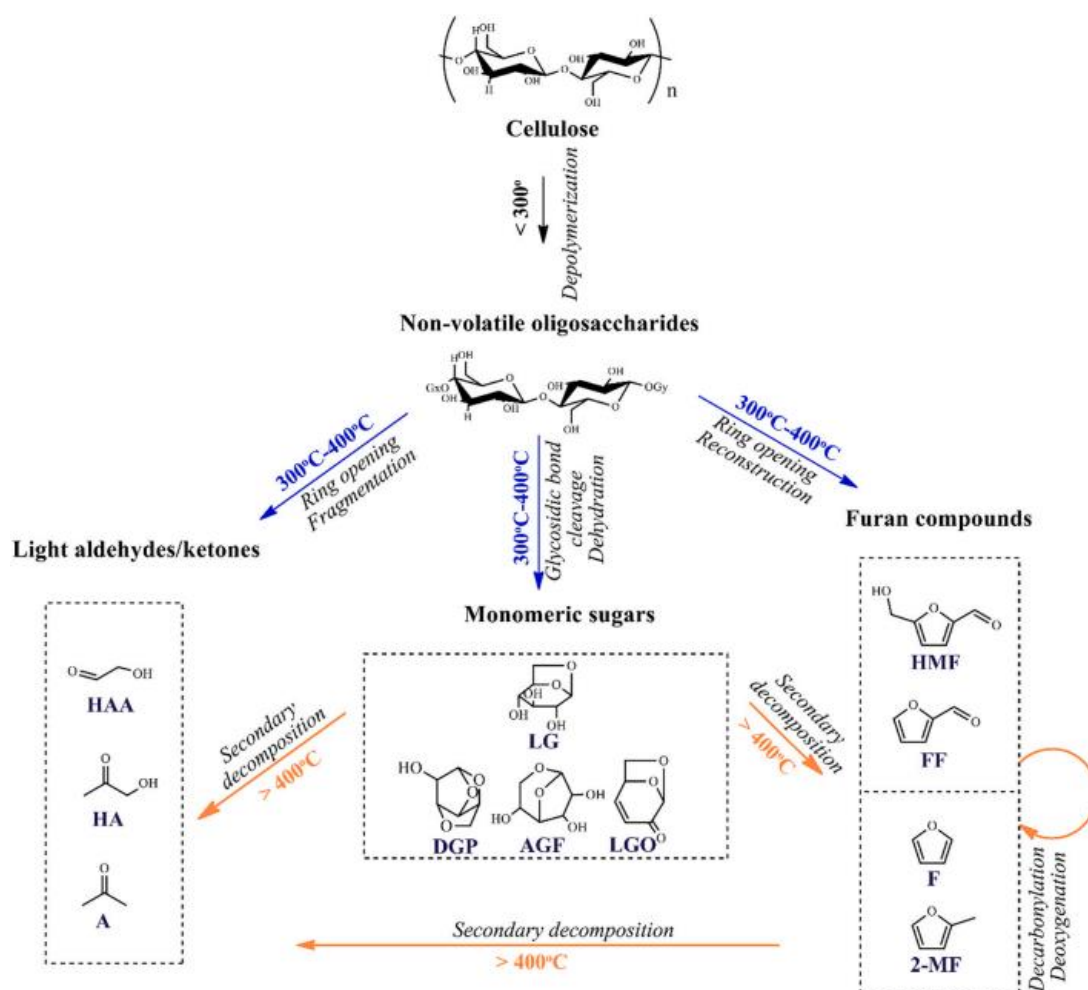


Figure 13 Pyrolysis behavior of lignin [6].

3.2 Pyrolysis process model

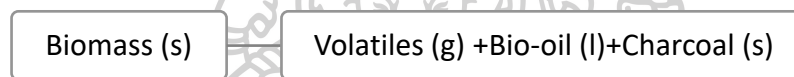
The pyrolysis process is modelled via the small and zero-dimensional biomass particle size without considering temperature change vs. distance or resistance from porous media. This study is primarily interested in kinetic chemical models that are simple and suited for initial evaluation, such as the single-particle model. Other processes and mechanisms (heat transfer and mass transfer) will be studied further, as well as equations for the conservation of mass and energy in each state of substance, and comprehensive equations of chemical reactions are studied. This study considers the flow of fluid around biomass particles, therefore the

equation of fluid from computational fluid dynamics models is considered as follows (Nakorn Tippayawong, Biomass Conversion Technology, pp. 268-269).

3.2.1 Kinetic chemical model

The thermal decomposition of biomass model divided into 3 types as follows.

- (i) One-step global models show that biomass pyrolysis yields volatiles (gases) and biochar which is solid material, and the decomposition of biomass also yields bio-oil during pyrolysis process. This model consider pyrolysis process as one-step 1st order reaction as follows:



By

$$\frac{d\alpha}{dt} = k(T) f(\alpha) \quad (1)$$

Where α is the extent of conversion

$f(\alpha)$ is the differential reaction model

$d\alpha/dt$ is the instantaneous rate of reaction

$k(T)$ is the rate constant expressed by eq.

$$k(T) = A \exp\left(\frac{-E_a}{RT}\right) \quad (2)$$

where A is the pre-exponential factor (1/s)

E_a is the activation energy (kJ/mol)

R is the universal gas constant (8.314 J/K.mol)

T is absolute temperature (K)

so

$$\frac{d\alpha}{dt} = A \exp\left(\frac{-E_a}{RT}\right) \cdot f(\alpha) \quad (3)$$

The extent of conversion can be expressed by Eq (4)

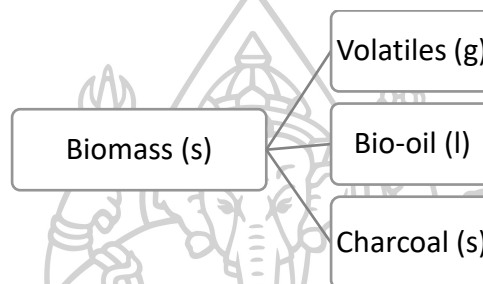
$$\alpha = \frac{m_o - m_i}{m_o - m_f} \quad (4)$$

where m_o is the initial mass

m_i is the instantaneous mass

m_f is the final mass after pyrolysis

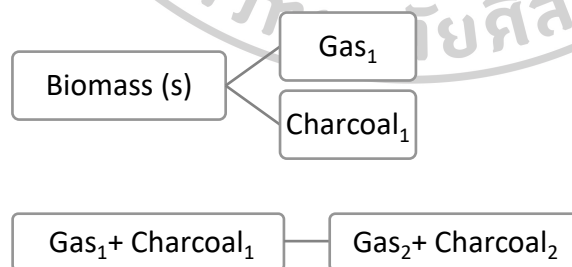
- (ii) One-step multi-reaction models consider pyrolysis as multiple first-order reactions occurring simultaneously in one step as follows.



By

$$\frac{dm_i}{dt} = -m_i A_i \exp\left(\frac{-E_i}{RT}\right) \quad (5)$$

- (iii) Two-step semi-global models considers pyrolysis process as a two-step first-order reaction followed by the products from the first step decomposed into the final product as follows.



By

$$\frac{dm_b}{dt} = -k_1 m_b^{n1} - k_2 m_b^{n2} \quad (6)$$

(7)

$$\frac{dm_{g1}}{dt} = k_1 m_b^{n1} - k_3 m_{g1}^{n3} m_{c1}^{n3}$$

$$\frac{dm_{c1}}{dt} = k_2 m_b^{n2} - k_3 m_{g1}^{n3} m_{c1}^{n3} \quad (8)$$

$$\frac{dm_{g2}}{dt} = k_3 m_{g1}^{n3} m_{c1}^{n3} \quad (9)$$

$$\frac{dm_{c2}}{dt} = \delta k_3 m_{g1}^{n3} m_{c1}^{n3} \quad (10)$$

Where m_b , m_{g1} , m_{g2} , m_{c1} , m_{c2} is biomass mass, gas₁, gas₂, and charcoal₁ charcoal₂, respectively.

K is rate constant of 1st-3rd reaction

n is order of 1st-3rd reaction

δ is conversion ratio of gas to charcoal

3.2.2 Single-particle model

Single-particle model studied the physical phenomena inside single biomass particle by considering biomass as porous cylindrical material and equations involving convection momentum, diffusion momentum and production of vapor, gas, water and energy as follows:

Gas pressure equation:

$$\frac{\partial P_g}{\partial t} - \frac{P_g}{T} \frac{\partial T}{\partial t} + \nabla \cdot \left(-\frac{P_g K}{T \mu} \nabla P_g \right) = \frac{R}{M_{mix}} (S_{evap} - S_{pyro}) \quad (11)$$

Vapor partial equation:

$$\frac{\partial P_v}{\partial t} - \frac{P_v}{T} \frac{\partial T}{\partial t} + \nabla \cdot \left(\frac{P_v}{T} \cdot \bar{u}_g \right) = \frac{R}{M_v} S_{evap} \quad (12)$$

Equation of continuity solid:

$$\frac{\partial \rho_i}{\partial t} = -S_{pyro} \quad (13)$$

Equation of continuity vapor:

$$\rho_w \frac{\partial S}{\partial t} \gamma = -S_{\text{evap}} \quad (14)$$

Energy equation:

$$\begin{aligned} \frac{\partial}{\partial t} [(\rho_g c_{pg} \gamma (1 - S) + \rho_w c_{pw} \gamma S + \rho_s c_{ps}) T] + \nabla (\rho_g c_{pg} \gamma (1 - S) \vec{u}_g T) \\ = \nabla k_{\text{mix}} (\nabla T) + S_{\text{evap}} h_{\text{evap}} + S_{\text{pyro}} h_{\text{pyro}} \end{aligned} \quad (15)$$

Darcy equation for velocity vector of gas:

$$\vec{u}_g = -\frac{K}{\mu_{\text{mix}} \gamma (1 - S)} \nabla P_g \quad (16)$$

Evaporation equation of water:

$$S_{\text{evap}} = a_v a_w (P_{\text{sat}} - P_v) \sqrt{\frac{M_v}{2\pi RT}} \quad (17)$$

Where K is resistance to viscosity (μ)

R is the universal gas constant

M_{mix} is the molar mass of mixture (air, gas and vapor)

M_v is molar mass of vapor

γ is porosity

c_p is specific heat

S is water saturation

k_{mix} is thermal conductive capacity of mixture

h is enthalpy

μ_{mix} is viscosity of mixture

a_v, a_w is vapor and water coefficients

Kinetic chemical model equation of biomass pyrolysis:

$$S_{\text{pyro}} = \sum k_i m_i \quad (18)$$

Where i is biomass component such as lignin, cellulose, and hemicellulose.

3.2.3 Computational fluid dynamic model

This model considers the interaction between biomass particles and surrounding gaseous fluid regardless of physical phenomena such as water and evaporation. The conservative equation and transport as follow:

$$\frac{\partial \gamma \rho_f}{\partial t} + \nabla \cdot (\rho_f \vec{u}) = S_{evap} + S_{pyro} \quad (19)$$

$$\frac{\partial (1 - \gamma) \rho_s}{\partial t} = -S_{evap} - S_{pyro} \quad (20)$$

$$\frac{\partial}{\partial t} (\gamma \rho_f \vec{u}) + \nabla \cdot (\rho_f \vec{u} \vec{u}) = -\nabla P + \nabla \cdot \tau - K \mu \vec{u} \quad (21)$$

$$\begin{aligned} \frac{\partial}{\partial t} (\gamma \rho_f c_{pf} T + (1 - \gamma) \rho_s c_{ps} T) + \nabla \cdot \vec{u} (\rho_f c_{pf} T + P) \\ = \nabla \cdot (k_{eff} \nabla T + (\tau \cdot \vec{u})) + S_{evap} h_{evap} + S_{pyro} h_{pyro} \end{aligned} \quad (22)$$

and

$$k_{eff} = \gamma k_f + (1 - \gamma) k_s \quad (23)$$

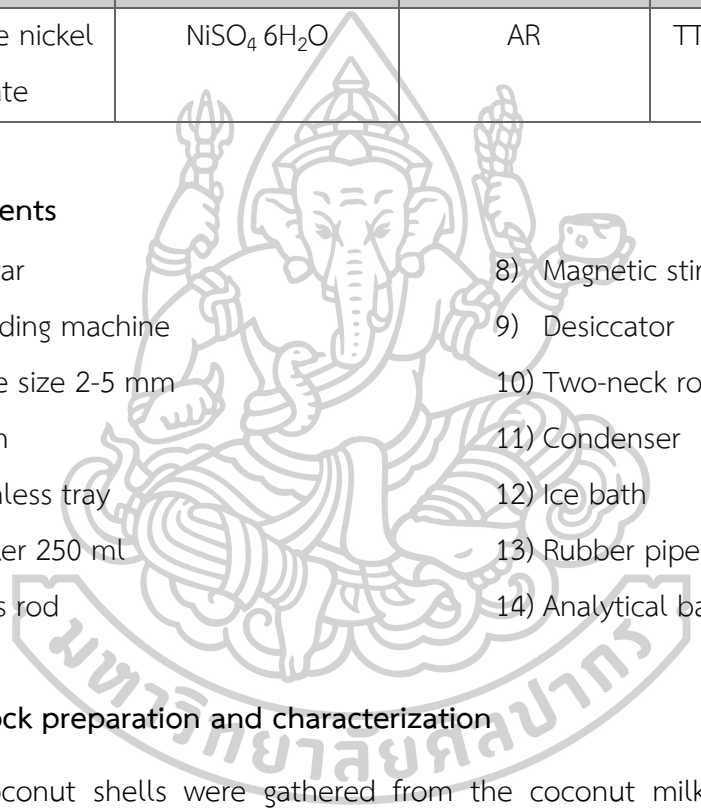
Chapter 4

Methodology

4.1 Chemical

Chemical	Formula	Grade	Manufacture
Activated carbon	-	Commercial	TTK science CO..LTD.
hexahydrate nickel sulphate	$\text{NiSO}_4 \cdot 6\text{H}_2\text{O}$	AR	TTK science CO..LTD.

4.2 Instruments

- 
- | | |
|----------------------|----------------------------------|
| 1) Mortar | 8) Magnetic stirrer |
| 2) Blending machine | 9) Desiccator |
| 3) Sieve size 2-5 mm | 10) Two-neck round bottom flasks |
| 4) Oven | 11) Condenser |
| 5) Stainless tray | 12) Ice bath |
| 6) Beaker 250 ml | 13) Rubber pipe |
| 7) Glass rod | 14) Analytical balance 4 digit |

4.3 Feedstock preparation and characterization

The coconut shells were gathered from the coconut milk factory in Muang district, Nakhon Pathom province, and then grinded using a mortar into small pieces before being cleaned with normal tap water and DI water. To eliminate moisture and other volatile contaminants, the cleaned coconut shells were dried in an oven at 105 °C for 24 hours. It was then crushed using a blender and sieved to particle sizes less than 250 µm. Flow chart 1 shows the feedstock preparation technique.

Proximate analysis of the coconut shell was analyzed according to ASTM D-271-48 standard to determine ash content, volatile matter, and fixed carbon. Elemental analysis was obtained by ThermoScientific CHNS elemental analyzer with combustion

technique. Oxygen content was calculated by the difference from the total compositions.

Flow chart 1. Procedure of feedstock Preparation.



1. Waste coconut shells were collected from coconut milk plant in Nakhon Pathom.



2. Coconut shells were washed and cleaned.



3. Coconut shells were dried in oven at 80 °C overnight to remove moisture.





4. Dried coconut shell was crushed in blending machine to get smaller size.



5. Crushed coconuts were sieved to get proper size in range of 2-5 mm.



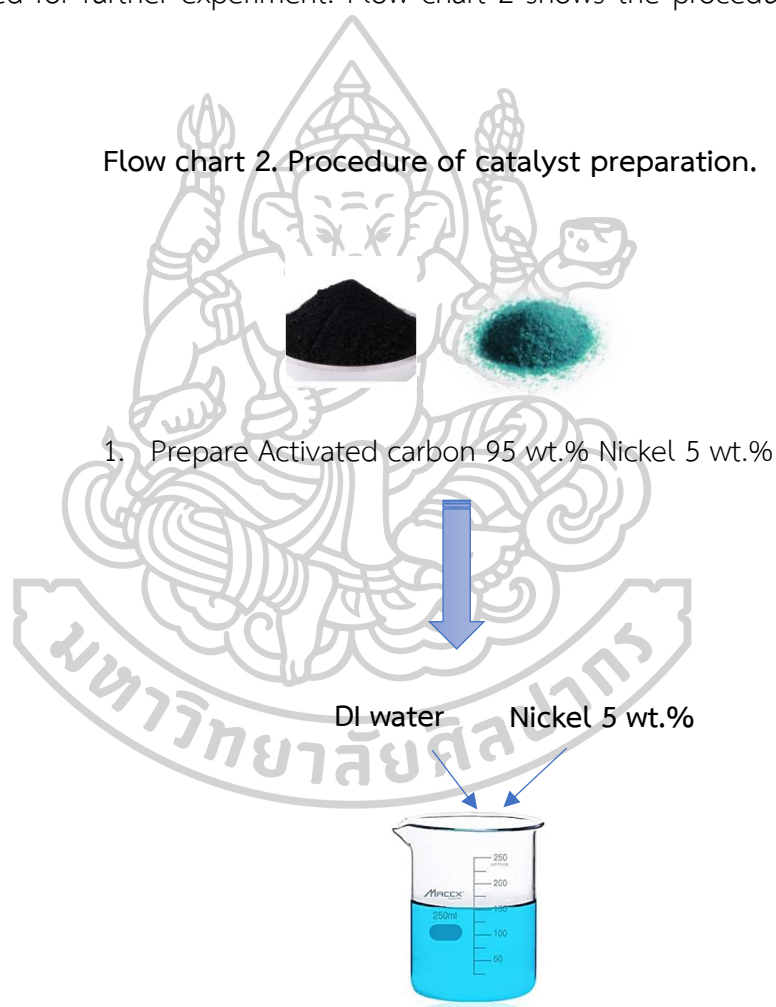
6. The feedstock was kept in desiccator for experiment.

4.4. Catalyst preparation and characterization

Commercial activated carbon (AC) with hexahydrate nickel sulphate ($\text{NiSO}_4 \cdot 6\text{H}_2\text{O}$). The impregnation approach was used to produce Ni-doped activated carbon catalysts with varying nickel loading amount of 0, 5, 10, 15, and 20 wt.% by using nickel sulphate hexahydrate as a precursor. The detailed preparation process of the

catalyst on AC was described as follows. Firstly, $\text{NiSO}_4 \cdot 6\text{H}_2\text{O}$ was dissolved and stirred in deionized water until a homogeneous solution was achieved. The AC was then impregnated with nickel sulphate solution and stirred at room temperature for 4 hours.; secondly, the excessive water was dried in the oven at $80\text{ }^\circ\text{C}$ overnight to remove internal moisture of the catalysts; at last, the dried Ni-doping AC catalyst was pyrolyzed under N_2 atmosphere pressures to target temperature $400\text{ }^\circ\text{C}$ with 30-minute holding time. These synthesized catalysts were then stored in a desiccator until required for further experiment. Flow chart 2 shows the procedure of catalyst preparation.

Flow chart 2. Procedure of catalyst preparation.

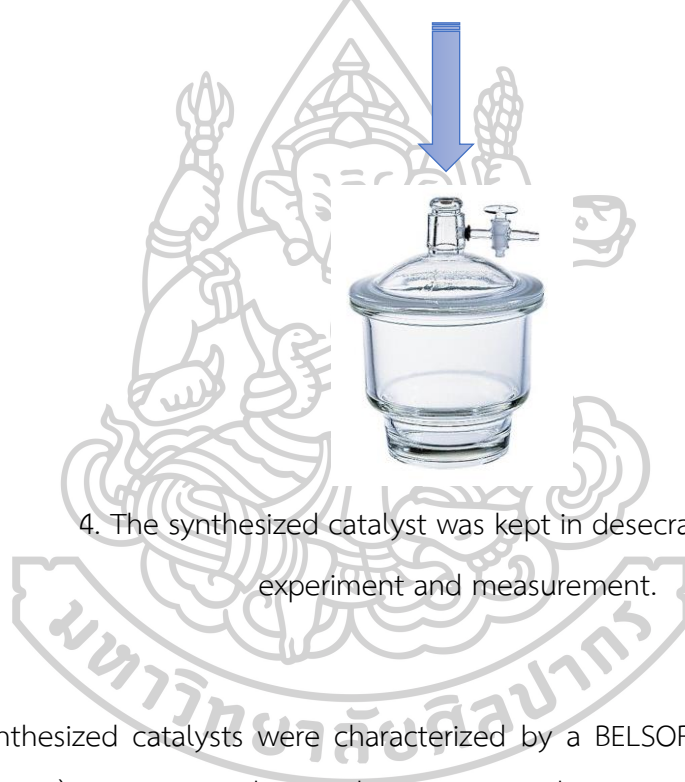


2. Ni was dissolved with DI water until homogeneous.





3. Adding activated carbon 95 wt.% into liquid Nickel 5 wt.% and stirrer for 4 hrs.



4. The synthesized catalyst was kept in desiccator for next experiment and measurement.

The synthesized catalysts were characterized by a BELSORP-mini II instrument (BEL Japan, Inc.) to support the catalytic activity. The N_2 sorption isotherm was examined to determine the surface area (BET technique) and pore volume/pore size (BJH method) of catalysts.

The XRD pattern of catalysts was obtained using Shimadzu Diffractometer XRD-6100 to verify the structural information of catalysts using X-ray operated at 40 kV accelerating voltage and 30 mA beam current with $CuK\alpha$ as radian source. Other settings were set to 2 (degree) in the range of 10° to 80° in 0.02° steps for 1s integration time per step as counting rate and $5^\circ/\text{min}$ as speed. The obtained XRD data were plotted by using Origin Pro to obtain XRD pattern.

The concentration of Nickel (Ni) element presented in prepared catalyst were determined and identified by using a MiniPal 4 X-ray fluorescence (XRF) spectrometer with a non-destructive analytical technique. XRF can detect elements ranging from Beryllium (BE) to Uranium (U) and beyond at trace levels and up to 100%. The XRF spectrometer detects the various component wavelengths of a sample's fluorescence emission when exposed to X-rays.

4.5. Experimental procedure

As shown in Fig 14, the catalytic pyrolysis of coconut shell was performed on a fix-bed reactor, operating at 300, 400 and 500 °C for 2 hr. with heating rate 12.33 °C/min under free-oxygen environment. 100 g of coconut shell and 10 g of the catalyst were separately packed with quartz wool in the reactor. During the operation, N₂ was used as a carrier gas with a gas flow rate 170 mL/min and connected at the bottom (inlet) of the reactor. Prior to the experiment, the reactor was purged with N₂ gas flow for approximately 5 minutes to remove the internal oxygen. The outlet of the reactor was connected to two condenser set-ups and both two condenser set-ups were connected to coolant. The bio-oil product was condensed in round bottom flasks in the ice bath. The gas product was released into the water bath and atmosphere. After the completion of the operation, the obtained biochar in the reactor was allowed to cool and then weighted to determine the product yield by using equation (24) and (25).

$$\mathbf{Weight}_{feedstock} = \mathbf{Weight}_{bio-oil} + \mathbf{Weight}_{char} + \mathbf{Weight}_{gas} \quad (24)$$

$$\mathbf{Product\ yield} = \frac{\mathbf{weight\ of\ each\ phase}}{\mathbf{weight\ of\ total\ product}} \times \mathbf{100} \quad (25)$$

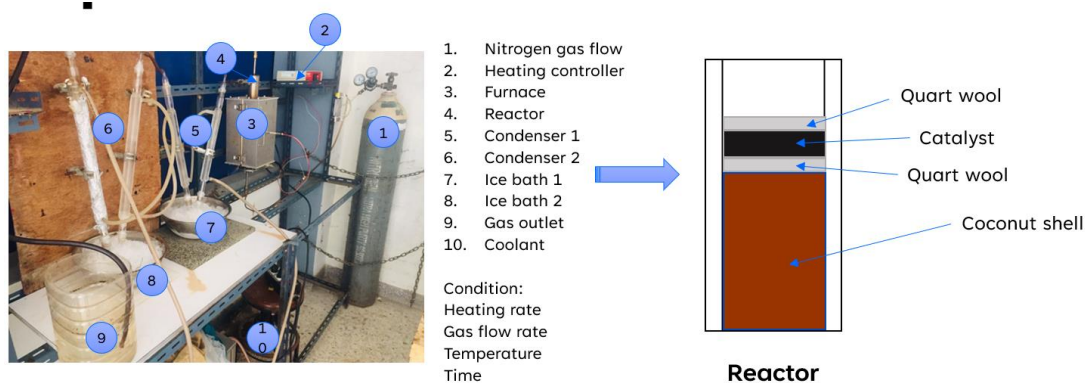


Figure 14 The experiment setup of catalytic pyrolysis of coconut shell.

4.6. Analysis of bio-oil and biochar

Thermo Scientific TSQ 9000 Triple Quadrupole GC-MS/MS equipment equipped with a TG-5SILMS column (30 m x 0.25 mm x 0.25 mm) was used to characterize the bio-oil compositions. As a carrier gas, helium (He) with a purity of 99.99% was used. The GC injection temperature was set to 290 °C for bio-oil vaporization and the He gas flow rate was set to 1 mL/min. The temperature of the GC oven was set at 40 °C for 1 minute, then raised to 300 °C for 10 minutes at a rate of 6 °C/min. The temperature of the mass spectrometer's ion source and transfer line was 200 °C. The GCMS spectra of each component in the bio-oil were compared to the mass spectral data from the National Institute of Standards and Technology (NIST).

The raw coconut shell and coconut biochar were analyzed by Fourier transform infrared (FT-IR) spectrometry using a Thermo ABS Nicolet IS5 FTIR Spectrometer with the attenuated total reflectance (ATR) technique in the wavenumber measurement range between 4000 and 500 cm^{-1} to confirm the transmittance spectrum of the sample and the existence of functional groups on raw coconut shell and biochar after catalytic pyrolysis.

Chapter 5

Results and Discussion

5.1 Characterization of Feedstock

The proximate and ultimate analysis of coconut shell (feed stock) used in this study, compared with other studies are shown in Table 4. It can be seen that most obtained values are varied due to differences in location, climate, and handling and storage [65]. The moisture content of coconut shell in this work shows the lowest moisture content of 2.90 wt.%, while the volatile contents are nearly similar for all samples in the range of 72.93-85.36 wt.%. It is important to note that higher volatile content in biomass results in a higher quantity of bio-oil and syngas. The ash content of coconut shell in this work was 1.80 wt.% which is lower than that of some other coconut shells (> 3.00 wt.%). For the ultimate analysis, it was found that the carbon content of the coconut shell used in this study was low, while the oxygen content was relatively high (high O/C). This may lead to the higher formation of gas-phase volatiles.



Table 4 Proximate and ultimate analysis of coconut shell from this work and literature (wt.% as dry).

Feedstocks	Proximate analyses			Ultimate analyses							Ref
	Moisture	Volatiles	Fixed carbon	Ash	C	H	N	S	O		
Coconut shell	2.90	74.06	21.24	1.80	47.79	5.86	0.11	00	46.24	This work	
Coconut shell	6.98	72.93	19.48	0.61	53.73	6.15	0.86	0.02	38.45	[66]	
Coconut shell	5.7	74.9	24.4	0.7	53.9	5.7	0.1	0.02	39.44	[67]	
Coconut shell	11.26	85.36	-	3.38	63.45	6.73	0.43	0.17	28.27	[68]	
Coconut shell	10.10	75.50	11.20	3.20	64.23	6.89	0.77	0.5	27.61	[69]	

5.2 Characterization of Catalyst

Surface characteristics of the catalysts were investigated with a N₂ adsorption-desorption technique, and the obtained result is shown in Table 5. As indicated, pure carbon with no Ni doping had a greater surface area (630 m²/g) than Ni-doped activated carbon with doping concentrations ranging from 5 to 20% (582-470 m²/g). The surface area and pore volume of the activated carbon support reduced dramatically as Ni loading increased, demonstrating that the surface area and pore structure of the support were impacted by Ni loading quantities and partly covered and occupied by the dispersed nickel species. Nickel molecules have a diameter of 0.250 nm. Because the average pore diameter of pure carbon is 3.8037 nm, nickel molecules can quickly enter the pores of activated carbon, reducing surface area, pore volume, and pore size.

Table 5 Physicochemical properties of the synthesized catalysts.

Catalyst	Surface area (m ² /g)	Pore volume (cm ³ /g)			Pore size (nm)
		meso	micro	total	
Pure carbon	630	0.3340	0.3315	0.5989	6.44
ACNi5%	582	0.2161	0.3871	0.5052	5.00
ACNi10%	554	0.1860	0.3749	0.4705	4.80
ACNi15%	536	0.1559	0.3445	0.4392	3.92
ACNi20%	470	0.1258	0.2552	0.3982	3.25

XRD characterization was performed to confirm the crystal structure of samples, as the result shown in Fig.5. Ni modification of activated carbon did not alter the activated carbon crystalline structure. As seen in Figure, the dominant peaks at 2 θ of 29.4, 43.94, 64.26, and 77.42 belong to activated carbon. The pattern is indexed to a rhombohedral R₃ space group, whereas the peaks at 2 θ of 44.5 (111), 52

(200), and 76.5 (220) correspond to Ni species [70, 71]. However, no notable peaks relating to Ni species were observed for any percentage of Ni doping, implying that Ni species in activated carbon were unable to be detected by XRD due to good dispersion on the high surface area of activated carbon support. This is in accordance with some literature, which has not found the metal species in support such activated carbon and HZSM-5 on XRD result [48, 52, 72] .

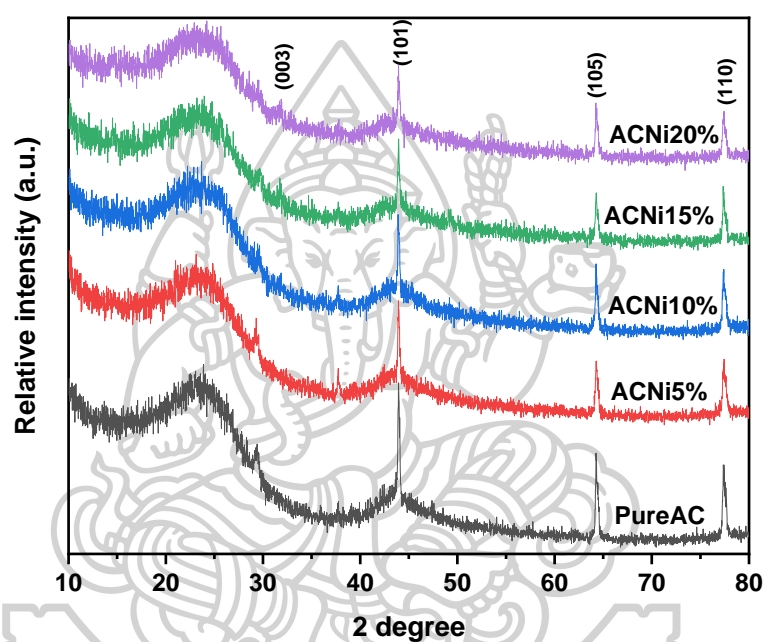


Figure 15 The XRD pattern of obtained Ni-doping activated carbon catalysts.

An XRF measurement was employed for determination of the Ni composition in the prepared catalysts, as the result shown in Table 6. The Ni concentrations were 0.0046, 5.87, 10.71, 15.33, and 21.61 wt.% in pure activated carbon, ACNi5, ACNi10%, ACNi10, and ACNi20%, respectively. The slightly higher Ni concentration in the prepared catalysts, which is more than the actual loading quantity, is due to heterogeneity error. The change in composition of the catalysts after the impregnation, for example water reduction, may be another reason for the higher Ni concentration.

Table 6 The concentration of Nickel element in prepared Ni-doped activated carbon catalyst (wt.%) obtained from XRF measurement.

Elemental compositions	Catalysts (wt.%)				
	Pure AC	ACNi5%	ACNi10%	ACNi15%	ACNi20%
Ni	0.046	5.87	10.71	15.33	21.61

5.3 Thermal pyrolysis

Thermal pyrolysis (no catalyst) of coconut shells was conducted at 300, 400 and 500 °C. The product yields from the pyrolysis are shown in Figure 16. It was found that the bio-oil yield and char yield at 300 °C was 38 and 42 wt.% respectively. Biochar yield at 300 °C was high due to the raw coconut shell wasn't completely pyrolyzed and the biochar has brown color of incomplete burnt biochar leading to less obtained bio-oil and gas yields. The bio-oil yield at 400 °C was 49 wt.% and char yield increased from 42 wt.% (at 300 °C) to 32 wt.% (at 400 °C), indicating the coconut shell was completely pyrolyzed at 400 °C resulting to the increasing of bio-oil yield and there was no brown color of coconut appear in the biochar. At 500 °C, the bio-oil yield decreased to 36 wt.% and gas yield was 35 wt.%. This is probably due to the secondary decomposition, turning condensable vapor into non-condensable product (gases). At 500 °C, the char yield slightly decreased to 29 wt.%, indicating that at 400 °C can achieve a complete pyrolyzed temperature. It can be concluded that 400 °C is the optimum pyrolysis temperature in this work with the highest bio-oil yields and less biochar and gas yields.

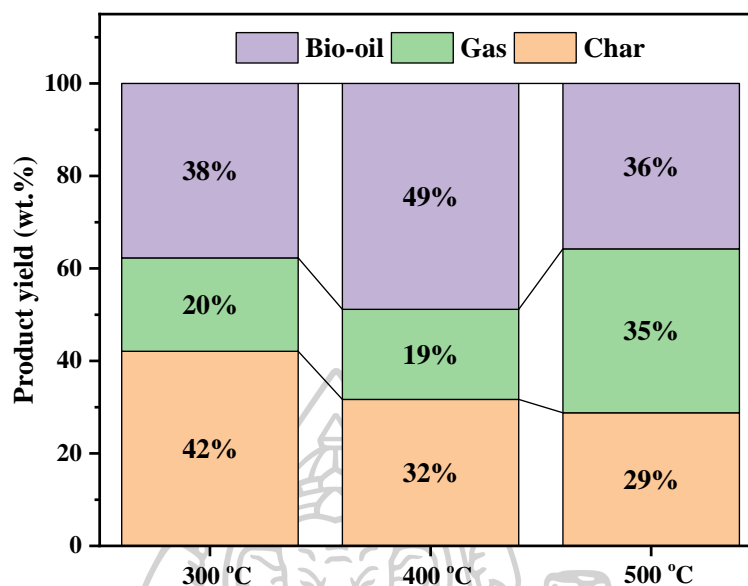


Figure 16 Thermal pyrolysis of coconut shells at 300, 400 and 500 °C.

5.4 Catalytic pyrolysis

Catalytic pyrolysis was conducted at the optimum temperature (400 °C) with 0-20 wt.% Ni-doped catalyst, as the result shown in Figure 17. With increasing Ni loading amount, the bio-oil yield decreased significantly from 49 wt.% to 37 wt.%. This suggests that the synthesized catalysts were quite successful in the bio-oil upgrading process, for enhancing the catalytic reactions which lead to the change of product distribution. However, the char yield is constant at 32 wt.% while the coke increases up to 12 wt.%. This suggests that a 10, 15 and 20 wt.% Ni overloads might increase metal sintering and coke deposition on the catalyst during the heat reaction process. The hydrocarbon molecule is then cracked into coke, increasing the carbon decomposition which can be assume coke according to other research [4] while the gas yield is almost constant at roughly 20 wt.%.

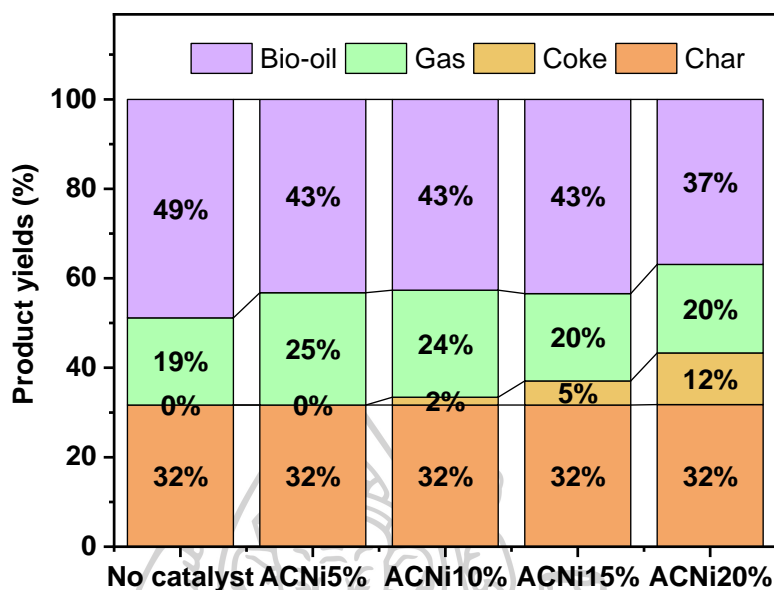


Figure 17 Mass balance of product yields obtained from pyrolysis/deoxygenation of coconut shell over 0-20%Ni-activated carbon catalyst at 400 °C.

The bio-oil production from the coconut of this study has been compared with the previous similar studies as shown in Table 7. The results shows that the coconut shell has the highest oil yield compared to other part of coconut such as coconut husk and pulp due to the coconut shell has higher lignin composition than hemicellulose and cellulose composition which leads to decomposition of lignin and produce high oil yield. In addition, it can be concluded that the optimized pyrolysis temperature for coconut shell should be in the range of 400-950 °C. Nevertheless, there are other factors that should be considered such as heating rate, gas flow rate, biomass pretreatment, type of reactor, catalyst and so on.

Table 7 Product distribution of catalytic pyrolysis of coconut shell without catalyst from this work and other literature.

Biomass	Temperature (°C)	Heating rate (°C/min)	Retention time (min)	Yield (wt.%)			Ref
				Char	Oil	Gas	
Coconut shell	400	12.33	30	32	49	19	This work
Coconut shell	950	10	-	34.6	25.5	26.3	[73]
Coconut shell	500	75	20	38.3	55.9	5.8	[74]
Coconut shell	615	175	20	32.4	61	6.6	[74]
Coconut shell	630	75	20	25.4	68.9	5.4	[74]
Coconut husk	950	11	-	28.3	17.3	26.9	[73]
Coconut pulp	700	80	9	16.56	-	83.44	[75]

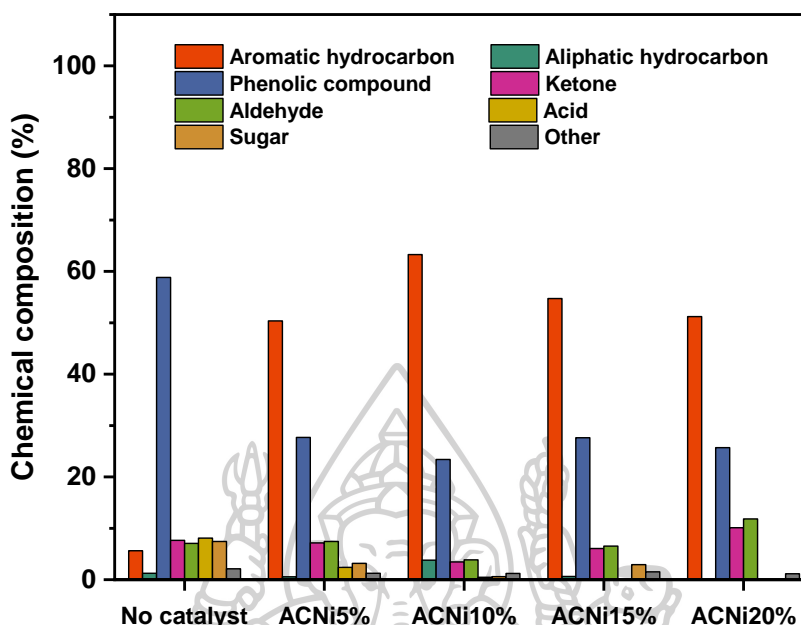


Figure 18 The chemical compositions of bio-oil obtained from pyrolysis/deoxygenation of coconut shell over 0-20%Ni-activated carbon catalyst.

The chemical composition of the obtained bio-oil with and without the catalysts was analyzed with a GC-MS technique. The detected compounds had been classified into 8 groups as shown in Figure 18. In general, biomass comprising hemicellulose, cellulose, and lignin is pyrolyzed to produce a range of oxygenated molecules such as anhydro sugar, carbonyl compounds, furans, phenol, and pyrans. These oxygenated molecules can be transformed into rich aromatic hydrocarbons, resulting in hydrocarbon conversion via some catalytic reactions (decarboxylation, dehydration, oligomerization, isomerization, dihydroxylation, and dehydrogenation).

In the absence of a Ni-doped catalyst, the total hydrocarbon content was 6.85 wt.%, the high phenol content was 58.82 wt.%, and acid and sugar were produced in the bio-oil. The total hydrocarbon content in the improved bio-oil increased considerably after utilizing a Ni-doped catalyst, notably aromatic hydrocarbon, since the high oxygenated components in the upgraded bio-oil were transformed into aromatic hydrocarbon. The total maximum hydrocarbon content of

67.06 wt.% in the upgraded bio-oil was obtained from 10% Ni-doped catalyst. Sugars in the upgraded bio-oils significantly decreased due to the transformation of furan compounds into aromatic hydrocarbons, while the observed reduction of acid was caused by the decarboxylation. It can also be seen that the total hydrocarbon content increases dramatically with Ni loading of 5-10 wt.%, especially aromatic hydrocarbons, from 5.62 to 63.26 wt.%. However, it conversely decreased when Ni loading increases by 15-20 wt.%, indicating that the appropriate Ni loading amount in this study should be 10% Ni-doped catalyst. It has been known that the mesoporous catalyst with pore sizes ranging from 2 to 5 nm exhibits high aromatic hydrocarbon selectivity. In this study, the 10% Ni-doped catalyst with suitable pore size 3.92 nm can provide sufficient mass transfer for reactant and product and the reactions within the pores, resulting in the conversion of oxygenated compounds with large molecule sizes into smaller hydrocarbons, and the synthesized Ni-doped catalyst has a high surface area (470-630 m²/g), resulting in an increase in active sites and a decrease in mass transfer resistance. Overloading Ni by 15-20% can lower total hydrocarbon content by inducing secondary processes in which hydrocarbon molecules break down into gases, coke, and other products over the extended residence time.



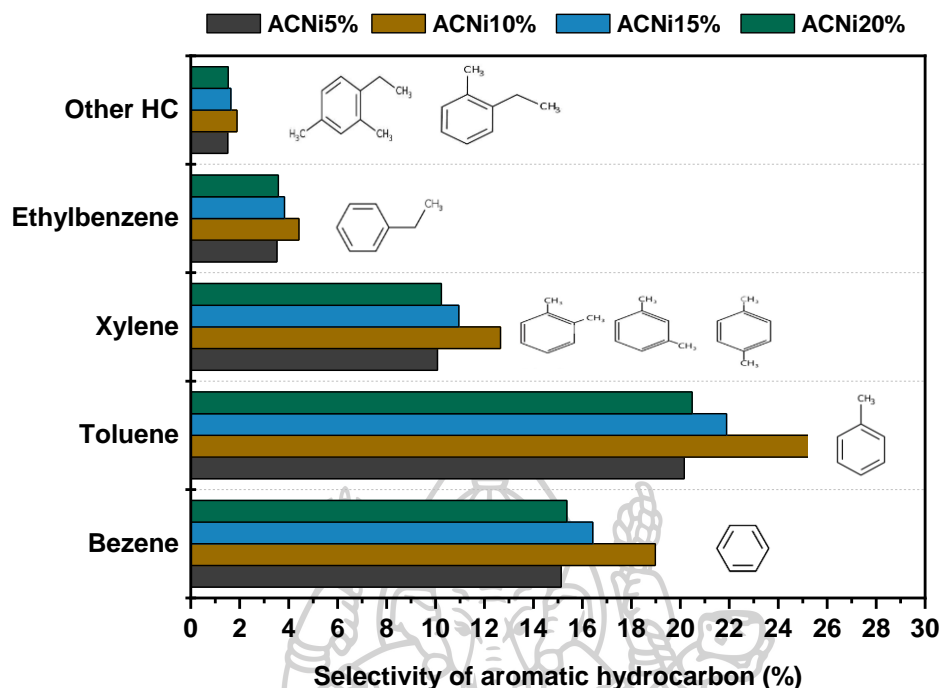


Figure 19 Aromatic selectivity of bio-oil obtained from pyrolysis/deoxygenation of coconut shell over 0-20%Ni-activated carbon catalyst.

Considering the aromatic hydrocarbon selectivity, the aromatic compounds were then classified into five types: benzene, toluene, xylene, ethylbenzene, and others as seen in Figure 19. The order of aromatic selectivity in the upgraded bio-oil was all the same with toluene > benzene > xylene > ethylbenzene. However, the amount of each compound varied among the catalysts, depending on various reactions, which favor generation of influenced including monocyclic aromatic hydrocarbons (MAHs). It should be noted that there were no reactions that can convert MAHs into polycyclic aromatic hydrocarbons (PAHs) such as naphthalene, pyrene, and indene, as seen that no PAHs like aromatization, polymerization, and oligomerization, had been observed.

The ability to promote aromatic selectivity of the catalysts used in this study and those of the others are compared in Table 8, along with their pyrolysis condition. This research shows that Ni doping carbon-based catalyst greatly improved phenol rich bio-oil into the higher yield and selectivity of aromatic hydrocarbons

under condition: temperature 400 °C, heating rate 12.33 °C/min and gas flow rate 170 mL/min. The bio-oil yield was steadily decreased with the increasing of Ni doping on activated carbon catalyst. But it shows that activated carbon catalyst doping with different amounts of Ni achieved aromatic yield up to 50-63% from 6%. Comparing with other studies, it exhibits that the catalysts used here provide the moderate aromatic selectivity, but have more benefit with the lower pyrolyzed temperature at 400 °C.



Table 8 Comparative study of various pyrolysis with different feedstock, catalyst, and conditions.

Feedstocks	Catalysts	Pyrolysis conditions				Aromatic content, %			Ref
		Temperature	Heating rate	Gas flow rate	Aromatic	Benzene	Toluene	Xylene	
		°C	°C/min	mL/min	yield, %				
Coconut shell	ACNi5%	400	12.33	170	50	15	20	10	
Coconut shell	ACNi10%	400	12.33	170	63	19	25	13	This
Coconut shell	ACNi15%	400	12.33	170	54	16.5	22	11	work
Coconut shell	ACNi20%	400	12.33	170	52	15.5	20.5	10.2	
Sunflower bio-oil	Al ₂ O ₃ -0.5	565	1000	100	42	23	27	10	[58]
Sunflower bio-oil	2.5%Zn/ Al ₂ O ₃ -0.5	565	1000	100	82	28	25	15	[58]
Sunflower bio-oil	2.5%Ni/Al ₂ O ₃ -0.5	565	1000	100	80	33	19	18	[58]
Palm kernel cake	15%Ni-AC	600	20	50	75	16	19	8	[4]
Palm Kernal cake	15%Fe-AC	600	20	50					[4]
Palm kernel cake	15%Cu-AC	600	20	50	65	-	-	-	[4]
Pine wood sawdust	HZSM-5-30	600	8.3	1200 sccm	11	23.1	30	13.9	[76]
Pine	Mo/ZSM-5	650	33.3	-	25.9	6.4	11.5	11.0	[77]
Pine	Co/ZSM-5	650	33.3	-	39.8	8	11.1	9.6	[77]
Pine	Ni/ZSM-5	650	33.3	-	41.3	7.4	10.6	10	[77]

Feedstocks	Catalysts	Pyrolysis conditions			Aromatic content, %			Ref	
		Temperature °C	Heating rate °C/min	Gas flow rate mL/min	Aromatic yield, %	Benzene	Toluene		Xylene
Pine	Pt/ZSM-5	650	33.3	-	46.4	6.7	12	11.9	[77]
Coconut shell	ZSM-5	500	10 C/s	200	20	-	-	-	[78]
Maple wood oil	ZSM-5	410			88.8	5.5	31.8	33.1	[79]
Cereal	ZSM-5	600		90	44.5	13.2	28	30	[80]
Beech	ZSM-5	650	20 °C/ms		23.7	12.3	28.6	23	[81]
Palm fruit +LDPE	No catalyst	550	10	250	13.71	-	-	-	[82]
Palm frond +LDPE	No catalyst	550	10	250	13.52	-	-	-	[82]
Sunflower stalks	0.5%Cu/HZSM-5	500	100 C/s	100	73	8	14	17	[48]

5.5 Characterization of Biochar

The FTIR spectra of raw coconut and coconut biochar after pyrolysis at 400 °C was shown in Figure 20. The FTIR spectra of both samples reveal the existence of different functional groups with either disappearance, reduction, or broadening of the peaks after pyrolysis. The O-H stretching vibration of hydroxyl groups was ascribed to the stretched broad band detected at 3340.59 cm⁻¹. The aliphatic C-H stretching of the CH, CH₂, and CH₃ groups caused the peak at 2905.72 cm⁻¹. For the peaks at 1733.80 and 1235.18 cm⁻¹, the C=C aromatic ring was observed. Peaks at 1160.46, 1032.21, and 769.46 cm⁻¹ were ascribed to Si-O stretching and bending, confirming silica present. C-O carboxyl groups and C-H stretching alkane or alkyl groups were ascribed to certain prominent measurable peaks at 1596.29 and 1371.62 cm⁻¹. After the catalytic pyrolysis, it was found that all the functional groups that originally existed in coconut shells had completely disappeared. A comparison table of wavenumber and functional group of each coconut char is shown in Table 9 [59, 60].

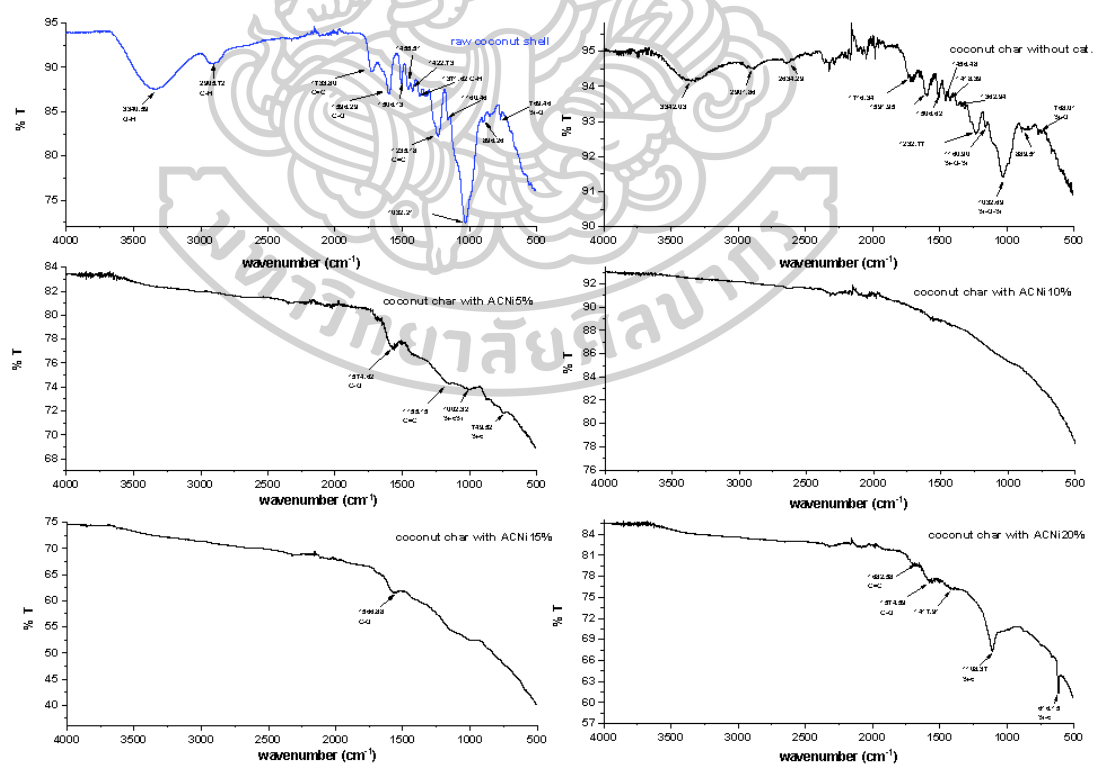


Figure 20 FTIR spectra of raw coconut shell and coconut chars with pyrolysis temperature, 400 °C.

Table 9 FTIR peak position comparison of raw coconut shell and other biochar after pyrolysis.

Functional group	Raw coconut			Coconut shell pyrolysis with				
	Raw coconut	No catalyst		ACNi5%	ACNi10%	ACNi15%	ACNi20%	
FTIR of peak positions (Wavenumber, cm ⁻¹)								
Hydroxyl group	3687.29-3000	3679-3000	-	-	-	-	-	-
Aliphatic group	2905.72	2901.86	-	-	-	-	-	-
Aromatic ring	1733.80, 1235.18	1716.34, 1231.77	0, 1155.15	-	-	-	1682.58	-
Carboxyl group	1596.29	1591.95	1574.62	-	-	1566.88	1574.59	-
Alkane or alkyl	1371.62	1362.94	-	-	-	-	-	-
Presence of silica	1160.46, 1032.21, 769.42	1160.90, 1032.69, 768.01	1002.32, 174.952	-	-	-	1108.37, 616.15	-

Chapter 6

Conclusions

5.1 Conclusion

The wet impregnation method was used to prepare a Ni-doped activated carbon catalyst with Ni loading amount of 5, 10, 15 and 20 wt.%. The coconut shell (CS) is used as biomass feedstock in catalytic pyrolysis for bio-oil production. The proximate analysis shows that the collected coconut shell has high volatile matter which relates to high bio-oil yield and less moisture and ash content compared to other coconut shells from different locations. The physicochemical properties of the prepared catalysts were analyzed. The surface area and pore size of prepared catalysts were in the range of 470-630 m²/g and 3.92-6.44 nm, respectively and decreased with the increasing of Ni loading amount. The XRD pattern showed Ni species unable to be detected by XRD due to good dispersion on the high surface area of activated carbon. The XRF shows the slight difference in the measured XRF value and actual value of Ni composition in prepared catalysts due to heterogeneity error and the change in composition of catalyst after impregnation. Under non-catalytic pyrolysis, the highest bio-oil yield was obtained at 400 °C. Under catalytic pyrolysis and pyrolysis temperature of 400 °C, the bio-oil yield decreased significantly with the increasing of Ni loading (wt.%) in prepared catalyst. The maximum total hydrocarbon yield of 67.06% and aromatic hydrocarbon yield of 63.26% were obtained by 10wt.%Ni-doped carbon catalyst. The bio-oil yield decreased significantly with the increasing of Ni loading amount due to the promoting of secondary reaction and deactivation of catalyst, resulting in an increase in coke yield. Catalysts with a Ni loading of 10% demonstrated the highest performance in terms of catalytic activity and selectivity for upgrading bio-oil. the aromatic selectivity was toluene > benzene > xylene > ethylbenzene. The FTIR result showed the existence, disappearance, and reduction of functional groups in raw CS and CS biochar. This

work proposed an acceptable technique for producing high-quality/yield bio-oil fuel at a cheap cost from waste biomass pyrolysis.

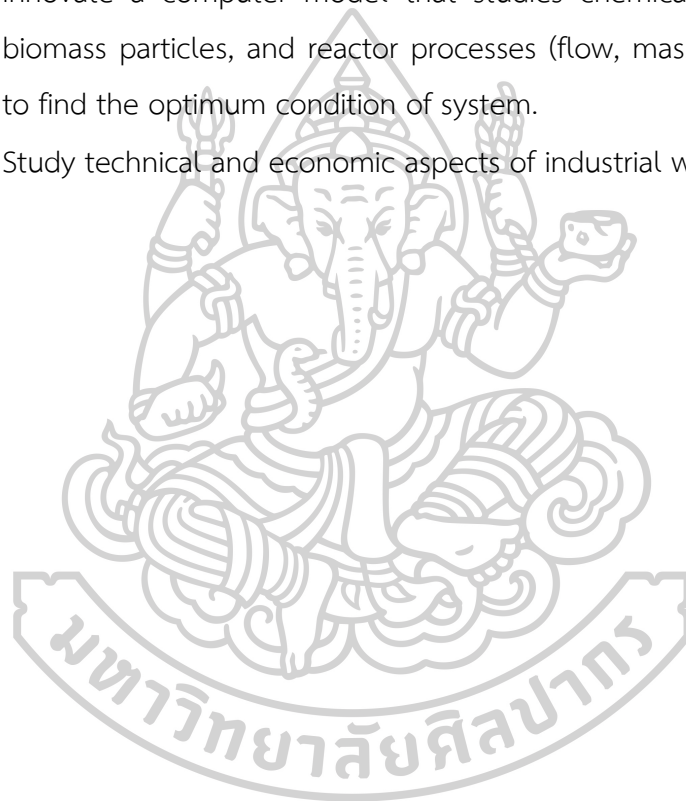
5.2 Suggestion

The pyrolysis of biomass to produce bio-oils is still in the early stages. This process makes it simple to produce liquid fuels with high bio-oil yields and cheap production costs. Bio-oil is low-grade liquid fuel as compared to petroleum fuel. Complications in multiphase structures, high oxygen, water, solids, and ash concentrations, low heating values, high viscosity and surface tension, chemical and thermal instability, low pH values, and poor igniting and combustion capabilities are poor characteristics of bio-oil. Despite their poor fuel features, bio-oils have several attractive properties. They are typically more lubricious, less poisonous, and more biodegradable than petroleum fuels. In this work need to further study more about fuel properties of bio-oil as mentioned above to consider the obtained bio-oil in this work to use as fuel. The biochar from coconut shell can be further studied on filtration and purification. Biochar is used as carbon sorbent and for mercury adsorption. The extraction of phenol from coconut shell bio-oil. Although there is many research and development on biomass pyrolysis in the recent year involving theoretical analysis, laboratory experiment, and commercial innovative development. But there are still some interesting challenges for more further research as follows:

- The application of various biomass and different pyrolysis reactor systems and scaling- up.
- Study on chemical mechanism to improve the reaction efficiency and disadvantage and advantages of various catalyst preparation methods.
- Research on catalytic biomass pyrolysis and the usage of gas produced from combustion as heating source.
- Study on multi-temperature step pyrolysis due to different temperatures are required to decompose the major biomass component such as

cellulose, hemicellulose and lignin so that the different products can be obtained separately.

- Develop standards according to fuel properties for bio-oil and biochar.
- Study on catalytic steam reforming to improve the pyrolysis process regarding the conversion of bio-oil into more valuable products such as high-quality chemicals and transportation fuel including gasoline, diesel, and jet fuel.
- Innovate a computer model that studies chemical reactions, kinetics, biomass particles, and reactor processes (flow, mass, and heat transfer) to find the optimum condition of system.
- Study technical and economic aspects of industrial work.



Appendix

1. Calculation of product yield from mass balance equation

$$\mathbf{Weight}_{feedstock} = \mathbf{Weight}_{bio-oil} + \mathbf{Weight}_{char} + \mathbf{Weight}_{gas}$$



Figure 1 Thermo Scientific TSQ 9000 Triple Quadrupole GC-MS/MS system



Figure 2 XRD-6100 X-Ray Diffractometer from Shimadzu



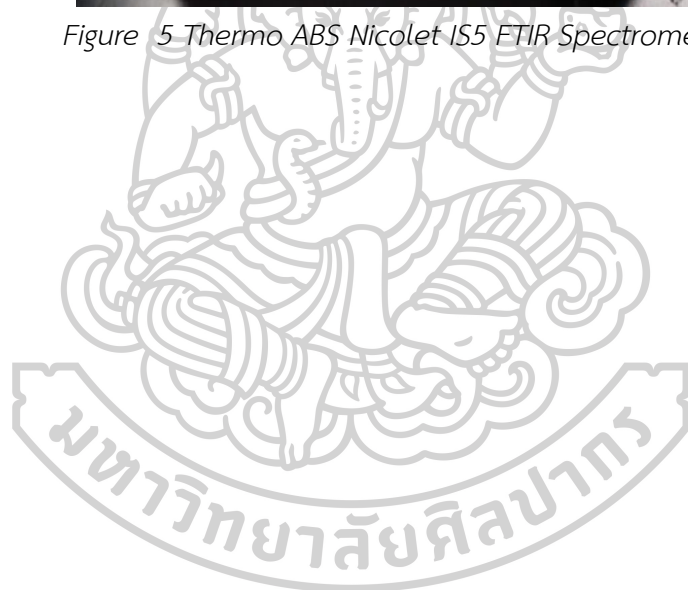
Figure 3 MiniPal 4 X-ray fluorescence (XRF) spectrometer



Figure 4 BELSORP-mini II instrument (BEL Japan, Inc.).



Figure 5 Thermo ABS Nicolet IS5 FTIR Spectrometer



REFERENCES

1. Tawalbeh, M., et al., *A critical review on metal-based catalysts used in the pyrolysis of lignocellulosic biomass materials*. Journal of Environmental Management, 2021. 299: p. 113597.
2. Amoako, G. and P. Mensah-Amoah, *Determination of calorific values of coconut shells and coconut husks*. 2018.
3. Qiu, B., et al., *Research progress in the preparation of high-quality liquid fuels and chemicals by catalytic pyrolysis of biomass: A review*. Energy Conversion and Management, 2022. 261: p. 115647.
4. Maneechakr, P. and S. Karnjanakom, *Improving the bio-oil quality via effective pyrolysis/deoxygenation of palm kernel cake over a metal (Cu, Ni, or Fe)-doped carbon catalyst*. ACS omega, 2021. 6(30): p. 20006-20014.
5. Dada, T.K., et al., *A review on catalytic pyrolysis for high-quality bio-oil production from biomass*. Biomass Conversion and Biorefinery, 2021: p. 1-20.
6. Hoang, A.T., et al., *Progress on the lignocellulosic biomass pyrolysis for biofuel production toward environmental sustainability*. Fuel Processing Technology, 2021. 223: p. 106997.
7. Azeta, O., et al., *A review on the sustainable energy generation from the pyrolysis of coconut biomass*. Scientific African, 2021. 13: p. e00909.
8. Ramanathan, A., et al., *Pyrolysis of waste biomass: Toward sustainable development. A Thermo-Economic Approach to Energy from Waste*; Elsevier: Amsterdam, The Netherlands, 2022.
9. Rathod, N., S. Jain, and M.R. Patel, *Thermodynamic analysis of biochar produced from groundnut shell through slow pyrolysis*. Energy Nexus, 2023. 9: p. 100177.
10. Abdullah, N., et al., *Banana pseudo-stem biochar derived from slow and fast pyrolysis process*. Heliyon, 2023: p. e12940.
11. Jokinen, N., et al., *Valorization potential of the aqueous products from*

- hydrothermal liquefaction and stepwise slow pyrolysis of wood bark and hemp hurds with yields and product comparison.* Bioresource Technology Reports, 2023: p. 101385.
12. Zha, Z., et al., *Effect of oxygen on thermal behaviors and kinetic characteristics of biomass during slow and flash pyrolysis processes.* Combustion and Flame, 2023. 247: p. 112481.
 13. Rubi, R.V., et al., *Slow pyrolysis of buri palm: Investigation of pyrolysis temperature and residence time effects.* Materials Today: Proceedings, 2023.
 14. Modak, S., et al., *Generation and characterization of bio-oil obtained from the slow pyrolysis of cooked food waste at various temperatures.* Waste Management, 2023. 158: p. 23-36.
 15. Huang, Y., et al., *Fast Pyrolysis Behaviors of Biomass with High Contents of Ash and Nitrogen Using TG-FTIR and Py-GC/MS.* Journal of Analytical and Applied Pyrolysis, 2023: p. 105922.
 16. Li, B., et al., *Oxidative fast pyrolysis of biomass in a quartz tube fluidized bed reactor: Effect of oxygen equivalence ratio.* Energy, 2023: p. 126987.
 17. Makepa, D.C., et al., *A systematic review of the techno-economic assessment and biomass supply chain uncertainties of biofuels production from fast pyrolysis of lignocellulosic biomass.* Fuel Communications, 2023: p. 100086.
 18. Zhang, C., et al., *Co-pyrolysis characteristics of camellia oleifera shell and coal in a TGA and a fixed-bed reactor.* Journal of Analytical and Applied Pyrolysis, 2021. 155: p. 105035.
 19. Meier, D., et al., *State-of-the-art of fast pyrolysis in IEA bioenergy member countries.* Renewable and Sustainable Energy Reviews, 2013. 20: p. 619-641.
 20. Mendoza-Martinez, C., et al., *Fast oxidative pyrolysis of eucalyptus wood residues to replace fossil oil in pulp industry.* Energy, 2023. 263: p. 126076.
 21. Alcazar-Ruiz, A., F. Dorado, and L. Sanchez-Silva, *Bio-phenolic compounds production through fast pyrolysis: Demineralizing olive pomace pretreatments.* Food and Bioproducts Processing, 2023. 137: p. 200-213.

22. Lu, Q., et al., *Mechanism of cellulose fast pyrolysis: The role of characteristic chain ends and dehydrated units*. Combustion and Flame, 2018. 198: p. 267-277.
23. Yang, H., et al., *Catalytic pyrolysis of cellulose with sulfonated carbon catalyst to produce levoglucosenone*. Fuel Processing Technology, 2022. 234: p. 107323.
24. Hameed, S., A. Sharma, and V. Pareek, *A distributed activation energy model for cellulose pyrolysis in a fluidized bed reactor*. Chemical Engineering Research and Design, 2023. 191: p. 414-425.
25. Sun, C., H. Tan, and Y. Zhang, *Simulating the pyrolysis interactions among hemicellulose, cellulose and lignin in wood waste under real conditions to find the proper way to prepare bio-oil*. Renewable Energy, 2023. 205: p. 851-863.
26. Genuino, H.C., et al., *Pyrolysis of LignoBoost lignin in ZnCl₂-KCl-NaCl molten salt media: Insights into process-pyrolysis oil yield and composition relations*. Journal of Analytical and Applied Pyrolysis, 2023: p. 106005.
27. Sangthong, S., et al., *Phenol-rich bio-oil from pyrolysis of palm kernel shell and its isolated lignin*. Industrial Crops and Products, 2022. 188: p. 115648.
28. Wang, L. and S.-T. Yang, *Solid state fermentation and its applications*. Bioprocessing for value-added products from renewable resources, 2007: p. 465-489.
29. Zaman, C.Z., et al., *Pyrolysis: a sustainable way to generate energy from waste*. Vol. 1. 2017: IntechOpen Rijeka, Croatia.
30. Verma, M., et al., *Biofuels production from biomass by thermochemical conversion technologies*. International Journal of Chemical Engineering, 2012. 2012.
31. Suntivarakorn, R., et al., *Fast pyrolysis from Napier grass for pyrolysis oil production by using circulating Fluidized Bed Reactor: Improvement of pyrolysis system and production cost*. Energy Reports, 2018. 4: p. 565-575.
32. Hossain, M. and P. Charpentier, *Hydrogen production by gasification of*

- biomass and opportunity fuels*, in *Compendium of Hydrogen Energy*. 2015, Elsevier. p. 137-175.
33. Plou, J., et al., *Experimental carbonation of CaO in an entrained flow reactor*. *Reaction Chemistry & Engineering*, 2019. 4(5): p. 899-908.
 34. Biagini, E., et al., *Development of an entrained flow gasifier model for process optimization study*. *Industrial & engineering chemistry research*, 2009. 48(19): p. 9028-9033.
 35. Maliutina, K., et al., *Comparative study on flash pyrolysis characteristics of microalgal and lignocellulosic biomass in entrained-flow reactor*. *Energy Conversion and Management*, 2017. 151: p. 426-438.
 36. Herod, A., et al., *Analytical methods for characterizing high-mass complex polydisperse hydrocarbon mixtures: an overview*. *Chemical Reviews*, 2012. 112(7): p. 3892-3923.
 37. Gupta, M., et al., *Flow characterization of moving and stirred bed vacuum pyrolysis reactor from RTD studies*. *Chemical Engineering Research and Design*, 2004. 82(1): p. 34-42.
 38. Jifara, B. and S. Mekuria, *Torrefaction of corncob and khat stem biomass to enhance the energy content of the solid biomass and parametric optimization*. *Bioresource Technology Reports*, 2023: p. 101381.
 39. Dong, N., et al., *Study on preparation of aromatic-rich oil by thermal dechlorination and fast pyrolysis of PVC*. *Journal of Analytical and Applied Pyrolysis*, 2023. 169: p. 105817.
 40. Djandja, O.S., et al., *Synthesis of N-doped carbon material via hydrothermal carbonization: Effects of reaction solvent and nitrogen source*. *Journal of Energy Storage*, 2023. 60: p. 106588.
 41. Ma, Y., et al., *Reactivity and performance of steam gasification during biomass batch feeding*. *Carbon Resources Conversion*, 2023.
 42. Soh, M., et al., *Role of levulinic acid in catalytic wet torrefaction of oil palm trunks: Insights into the hydrochar physicochemical properties, liquid phase composition, and reaction mechanisms*. *Process Safety and Environmental Protection*, 2023.

43. Lee, C.S., A.V. Conradie, and E. Lester, *The integration of low temperature supercritical water gasification with continuous in situ nano-catalyst synthesis for hydrogen generation from biomass wastewater*. Chemical Engineering Journal, 2023. 455: p. 140845.
44. Sanito, R.C., et al., *Volatile organic compounds (VOCs) analysis from plasma pyrolysis of printed circuit boards (PCB) with the addition of CaCO₃ from natural flux agents*. Environmental Technology & Innovation, 2023: p. 103011.
45. Nachenius, R.W., et al., *Biomass pyrolysis*, in *Advances in chemical engineering*. 2013, Elsevier. p. 75-139.
46. Dong, S., et al., *Catalytic conversion of model compounds of plastic pyrolysis oil over ZSM-5*. Applied Catalysis B: Environmental, 2023. 324: p. 122219.
47. Tshabalala, T.E. and M.S. Scurrrell, *Aromatization of n-hexane over Ga, Mo and Zn modified H-ZSM-5 zeolite catalysts*. Catalysis Communications, 2015. 72: p. 49-52.
48. Chaihad, N., et al., *In-situ catalytic upgrading of bio-oil derived from fast pyrolysis of sunflower stalk to aromatic hydrocarbons over bifunctional Cu-loaded HZSM-5*. Journal of Analytical and Applied Pyrolysis, 2021. 155: p. 105079.
49. Veses, A., et al., *Catalytic upgrading of biomass derived pyrolysis vapors over metal-loaded ZSM-5 zeolites: Effect of different metal cations on the bio-oil final properties*. Microporous and Mesoporous Materials, 2015. 209: p. 189-196.
50. Vichaphund, S., et al., *Production of aromatic compounds from catalytic fast pyrolysis of Jatropha residues using metal/HZSM-5 prepared by ion-exchange and impregnation methods*. Renewable energy, 2015. 79: p. 28-37.
51. Peng, H., et al., *Intra-crystalline mesoporous zeolite encapsulation-derived thermally robust metal nanocatalyst in deep oxidation of light alkanes*. Nature Communications, 2022. 13(1): p. 295.

52. Karnjanakom, S., et al., *High selectivity and stability of Mg-doped Al-MCM-41 for in-situ catalytic upgrading fast pyrolysis bio-oil*. Energy Conversion and Management, 2017. 142: p. 272-285.
53. Zhao, M., N.H. Florin, and A.T. Harris, *The influence of supported Ni catalysts on the product gas distribution and H₂ yield during cellulose pyrolysis*. Applied Catalysis B: Environmental, 2009. 92(1-2): p. 185-193.
54. Iliopoulou, E., et al., *Catalytic pyrolysis of olive mill wastes towards advanced bio-fuels and bio-chemicals using metal oxide catalysts*. Catalysis Today, 2023: p. 114151.
55. Yan, X., et al., *A comparison of Al₂O₃ and SiO₂ supported Ni-based catalysts in their performance for the dry reforming of methane*. Journal of Fuel Chemistry and Technology, 2019. 47(2): p. 199-208.
56. Zheng, Y., D. Chen, and X. Zhu, *Aromatic hydrocarbon production by the online catalytic cracking of lignin fast pyrolysis vapors using Mo₂N₃/Al₂O₃*. Journal of Analytical and Applied Pyrolysis, 2013. 104: p. 514-520.
57. Zhao, W., et al., *Promotion effects of SiO₂ or/and Al₂O₃ doped CeO₂/TiO₂ catalysts for selective catalytic reduction of NO by NH₃*. Journal of hazardous materials, 2014. 278: p. 350-359.
58. Karnjanakom, S., et al., *Selectively catalytic upgrading of bio-oil to aromatic hydrocarbons over Zn, Ce or Ni-doped mesoporous rod-like alumina catalysts*. Journal of Molecular Catalysis A: Chemical, 2016. 421: p. 235-244.
59. Yuan, C., et al., *High-grade biofuel production from catalytic pyrolysis of waste clay oil using modified activated seaweed carbon-based catalyst*. Journal of Cleaner Production, 2021. 313: p. 127928.
60. Di Stasi, C., et al., *Optimization of the operating conditions for steam reforming of slow pyrolysis oil over an activated biochar-supported Ni-Co catalyst*. International Journal of Hydrogen Energy, 2021. 46(53): p. 26915-26929.
61. Suriapparao, D.V. and R. Vinu, *Resource recovery from synthetic polymers*

- via microwave pyrolysis using different susceptors*. Journal of analytical and applied pyrolysis, 2015. 113: p. 701-712.
62. Fan, L., et al., *Screening microwave susceptors for microwave-assisted pyrolysis of lignin: Comparison of product yield and chemical profile*. Journal of Analytical and Applied Pyrolysis, 2019. 142: p. 104623.
63. Omoriyekomwan, J.E., A. Tahmasebi, and J. Yu, *Production of phenol-rich bio-oil during catalytic fixed-bed and microwave pyrolysis of palm kernel shell*. Bioresource technology, 2016. 207: p. 188-196.
64. Lam, S.S., et al., *Recovery of diesel-like fuel from waste palm oil by pyrolysis using a microwave heated bed of activated carbon*. Energy, 2016. 115: p. 791-799.
65. Danish, M., et al., *Characterization of South Asian agricultural residues for potential utilization in future 'energy mix'*. Energy Procedia, 2015. 75: p. 2974-2980.
66. Walters, R.C., E.H. Fini, and T. Abu-Lebdeh, *Enhancing asphalt rheological behavior and aging susceptibility using bio-char and nano-clay*. Am. J. Eng. Appl. Sci, 2014. 7(1): p. 66-76.
67. Mohammad, L., M. Elseifi, and S. Cooper. *Laboratory Evaluation of Asphalt Mixtures Containing Bio-binder Technologies [C/CD]*. in *TRB 2013 Annual Meeting CD-ROM*. 2013.
68. Huang, S.-C., D. Salomon, and J.E. Haddock, *Alternative Binders for Sustainable Asphalt Pavements: Papers from a Workshop*. *Workshop Introduction*. Transportation Research Circular, 2012(E-C165).
69. Dongardive, S., A. Mohod, and Y. Khandetod, *Slow pyrolysis of coconut shell to produce crude oil*. Int J Innov Eng Technol, 2019. 12(3): p. 94-97.
70. Aboud, M.F.A., et al., *Hydrogen storage in pristine and d10-block metal-anchored activated carbon made from local wastes*. Energies, 2015. 8(5): p. 3578-3590.
71. Zieliński, M., et al., *Hydrogen storage in nickel catalysts supported on activated carbon*. International journal of hydrogen energy, 2007. 32(8): p.

- 1024-1032.
72. Sofyan, N., et al. *Use of carbon pyrolyzed from rice husk in LiFePO₄/V/C composite and its performance for lithium ion battery cathode*. in *IOP Conference Series: Earth and Environmental Science*. 2018. IOP Publishing.
 73. Wang, Q. and J. Sarkar, *Pyrolysis behaviors of waste coconut shell and husk biomasses*. *Towards Energy Sustainability*, 2018. 111.
 74. Siengchum, T., M. Isenberg, and S.S. Chuang, *Fast pyrolysis of coconut biomass—An FTIR study*. *Fuel*, 2013. 105: p. 559-565.
 75. Pantas, P.M.B.M.P., *Thermogravimetric analysis of rice husk and coconut pulp for potential biofuel production by flash pyrolysis*. *Malaysian Journal of Analytical Sciences*, 2014. 18(3): p. 705-710.
 76. Carlson, T.R., et al., *Production of green aromatics and olefins by catalytic fast pyrolysis of wood sawdust*. *Energy & Environmental Science*, 2011. 4(1): p. 145-161.
 77. Thangalazhy-Gopakumar, S., S. Adhikari, and R.B. Gupta, *Catalytic pyrolysis of biomass over H⁺ ZSM-5 under hydrogen pressure*. *Energy & fuels*, 2012. 26(8): p. 5300-5306.
 78. Wei, X., et al., *High-grade bio-oil produced from coconut shell: a comparative study of microwave reactor and core-shell catalyst*. *Energy*, 2020. 212: p. 118692.
 79. Adjaye, J.D., S.P. Katikaneni, and N.N. Bakhshi, *Catalytic conversion of a biofuel to hydrocarbons: effect of mixtures of HZSM-5 and silica-alumina catalysts on product distribution*. *Fuel Processing Technology*, 1996. 48(2): p. 115-143.
 80. Wang, K. and R.C. Brown, *Catalytic pyrolysis of corn dried distillers grains with solubles to produce hydrocarbons*. *ACS Sustainable Chemistry & Engineering*, 2014. 2(9): p. 2142-2148.
 81. Li, J., et al., *Catalytic fast pyrolysis of biomass with mesoporous ZSM-5 zeolites prepared by desilication with NaOH solutions*. *Applied Catalysis A: General*, 2014. 470: p. 115-122.
 82. Al-Maari, M., et al., *Co-pyrolysis of oil palm empty fruit bunch and oil*

palm frond with low-density polyethylene and polypropylene for bio-oil production. Arab J Chem 14: 103282. 2021.





VITA

NAME ไอยรินทร์ ทองแดง

DATE OF BIRTH 10 ธันวาคม 2539

PLACE OF BIRTH ราชบุรี, ไทย

INSTITUTIONS ATTENDED วิศวกรรมศาสตรมหาบัณฑิต วิศวกรรมเคมี

HOME ADDRESS 12 สนามจันทร์คอร์ท ต. สนามจันทร์ อ. เมือง จ.นครปฐม 73000

PUBLICATION

Effect of Gd₂O₃ in Li₂O–AlF₃–CaF₂–P₂O₅–Eu₂O₃ glasses for laser medium and X-rays detection material applications
CS Sarumaha, J Rajagukguk, J Tongdang, N Chanthima, HJ Kim, ...Radiation Physics and Chemistry 199, 110362

White Emission from Li₂O–BaO–Bi₂O₃–P₂O₅ Glass Doped with Dy³⁺ for Optical Condensed Material Applications
J Tongdang, N Chanthima, N Kiwsakunkarn, Y Tariwong, ...Integrated Ferroelectrics 223 (1), 18-28

Eu³⁺ ions doped lithium aluminium gadolinium borophosphate glasses: Energy transfer, optical and luminescence behaviors for red emission material
N Kiwsakunkran, J Tongdang, N Chanthima, HJ Kim, S Kothan, ...Radiation Physics and Chemistry 199, 110390

Investigation on structural and compositional properties of natural amethyst
J Tongdang, Y Tariwong, N Chanthima The 13th NPRU National Academic Conference Nakhon Pathom Rajabhat University

Determination of Radiation Attenuation Coefficient on
Lithium Barium Bismuth Phosphate Glasses at 662 keV
N Chanthima, J Tongdang, S Reungsri, J Kaewkhao

Study on Optical Properties of Lithium Barium Bismuth
Phosphate Glasses Doped with Sm^{3+} ions
N Chanthima, J Tongdang, S Reungsri, J Kaewkhao

